

TEST REPORT

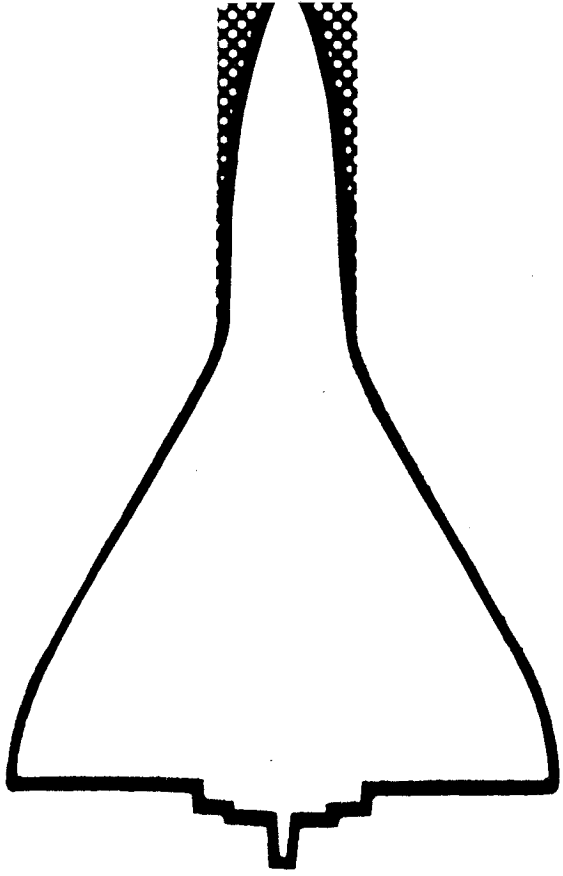
DETERMINATION OF THE RELATIVE RESISTANCE TO IGNITION  
OF SELECTED TURBOPUMP MATERIALS IN  
HIGH-PRESSURE, HIGH-TEMPERATURE, OXYGEN ENVIRONMENTS

(NASA-CR-179505-Vol-1) DETERMINATION OF THE  
RELATIVE RESISTANCE TO IGNITION OF SELECTED  
TURBOPUMP MATERIALS IN HIGH-PRESSURE,  
HIGH-TEMPERATURE, OXYGEN ENVIRONMENTS,  
VOLUME 1 Interim Report (NASA) 75 p

N89-16003

Unclas

G3/25 0185103



Lyndon B. Johnson Space Center  
**White Sands Test Facility**  
Post Office Drawer MM  
Las Cruces, New Mexico 88004  
AC 505 524-5011

TEST REPORT  
DETERMINATION OF THE RELATIVE RESISTANCE TO IGNITION  
OF SELECTED TURBOPUMP MATERIALS IN  
HIGH-PRESSURE, HIGH-TEMPERATURE, OXYGEN ENVIRONMENTS

Issued By  
National Aeronautics and Space Administration  
Johnson Space Center  
White Sands Test Facility  
Laboratories Test Office

Prepared By: Joel M. Stoltzfus  
Joel M. Stoltzfus, Lockheed-EMSCO

Prepared By: Frank J. Benz  
Frank J. Benz/RF  
NASA Laboratories Test Office

Approved By: Frank J. Benz  
David L. Phippen, Chief  
NASA Laboratories Test Office

## ABSTRACT

Advances in the design of the liquid oxygen, liquid hydrogen engines for the Space Transportation System call for the use of warm, high-pressure oxygen as the driving gas in the liquid oxygen turbopump. The NASA Lewis Research Center requested the NASA White Sands Test Facility (WSTF) to design a test program to determine the relative resistance to ignition of nine selected turbopump materials: Hastelloy X, Inconel 600, Invar 36, Monel K-500, Monel 400, nickel 200, silicon carbide, stainless steel 316, and zirconium copper. The materials were subjected to particle impact and to frictional heating in high-pressure oxygen.

In the particle impact tests, nickel 200, Monel 400, and silicon carbide were the most resistant to ignition; Monel K-500 and zirconium copper were slightly less resistant to ignition; and Hastelloy X, Invar 36, and stainless steel 316 were the least resistant to ignition. Inconel 600 was not tested.

In frictional heating tests of pairs of like materials, the ranking was generally upheld, with the materials ranked in order of decreasing resistance to ignition as follows: nickel 200, Inconel 600, Monel 400, Monel K-500, Hastelloy X, Invar 36, and stainless steel 316. Pairs of silicon carbide and zirconium copper failed mechanically at modest contact pressures and did not ignite.

In tests where pairs of different materials were rubbed together, the material rated less resistant to ignition in previous tests appeared to control the resistance to ignition of the pair.

Tests designed to determine the effects of oxygen pressure on the results of frictional heating appeared to indicate that the greater heat rates per unit area required to ignite metals at high pressures resulted from increased convective heat losses from the test samples.

## PREFACE

This interim report addresses the test series that resulted from three test plans written at the NASA White Sands Test Facility in response to a request from the NASA Lewis Research Center to determine the relative compatibility of selected turbopump materials in gaseous oxygen. The first test plan, Determination of the Ignition Sensitivity of Selected Turbopump Metals in High Pressure, High Temperature, Oxygen Environments (TP-WSTF-324), proposed tests in which eight materials were impacted with particles in hot, high-pressure oxygen and nine materials were heated frictionally in high-pressure oxygen. The second test plan, TP-WSTF-324 ADDI, proposed tests in which pairs of different materials were rubbed together in high-pressure oxygen to induce frictional heating. The third test plan, Evaluation of Pressure Effects in the WSTF Friction Rubbing Test System (TP-WSTF-356), proposed tests to determine the effects of the test gas pressure on the results of frictional heating tests. Testing proposed in the first and third test plans has been completed, and six of the eight tests proposed in the second test plan have been completed.

## TABLE OF CONTENTS

Section	Page
VOLUME I	
LIST OF FIGURES	v
LIST OF TABLES	vii
1.0 INTRODUCTION	1
2.0 OBJECTIVES	2
3.0 PARTICLE IMPACT TESTS	2
3.1 BACKGROUND	3
3.2 TEST SYSTEM DESCRIPTION	4
3.3 TEST CONSIDERATIONS	7
3.3.1 Sample Preparation	
3.3.2 Test Conditions	
3.3.3 Test Procedure	
3.4 PARTICLE IMPACT TEST RESULTS	10
3.4.1 Tests With Impact Plates	
3.4.1.1 Types of Ignition Events Observed	
3.4.1.2 Ignition Susceptibility of the Materials	
3.4.1.3 Discussion of Test Results	
3.4.2 Tests With Rupture Disks	
3.4.2.1 Types of Ignition Events Observed	
3.4.2.2 Ignition Susceptibility of the Materials	
3.4.2.3 Discussion	
4.0 FRICTIONAL HEATING TESTS	19
4.1 BACKGROUND	19
4.2 TEST SYSTEM DESCRIPTION	22
4.3 TEST CONSIDERATIONS	26
4.3.1 Sample Preparation	
4.3.2 Test Conditions	
4.3.3 Test Procedure	
4.4 FRICTIONAL HEATING TEST RESULTS	29
4.4.1 Ignition Resistance of Pairs of Like Materials	
4.4.1.1 General Comments Concerning the Data	
4.4.1.2 Relative Resistance of the Test Materials to Ignition	
4.4.1.3 Discussion of Test Results	
4.4.2 Ignition Resistance of Pairs of Different Materials	
4.4.2.1 General Comments Concerning the Data	
4.4.2.2 Relative Resistance of the Test Materials to Ignition	
4.4.2.3 Discussion of the Test Results	

## TABLE OF CONTENTS (Continued)

Section	Page
4.4.3	Effect of Oxygen Pressure on the Ignition of Materials
4.4.3.1	General Comments Concerning the Data
4.4.3.2	Description of the Test Results
4.4.3.3	Discussion of the Test Results
5.0	CONCLUSIONS 56
	LIST OF REFERENCES 58
	DISTRIBUTION 60
APPENDIX A:	Temperature Calibration of Particle Impact Tester A-1
APPENDIX B:	Estimation of Minimum Particle Velocity by a Dent-Block Comparison Test B-1
VOLUME II	
APPENDIX C:	Data From Particle Impact Test C-1
APPENDIX D:	Data From Frictional Heating Tests on Pairs of Like Materials D-1
VOLUME III	
APPENDIX E:	Data From Frictional Heating Tests on Pairs of Different Materials E-1
VOLUME IV	
APPENDIX F:	Data From Frictional Heating Tests to Determine the Effect of Oxygen Pressure on the Pv Product Required for Ignition F-1

## LIST OF FIGURES

Figure	Page
1. Schematic Diagram of the Gaseous Oxygen Test System with the Particle Impact Chamber Installed	5
2. Cross-Sectional View of the Particle Impact Test Chamber Showing Two Target Configurations	6
3. Impact Plates Showing (a) No Burning, (b) Slight Evidence of Burning, and (c) Partial Burning	11
4. End View of a Test Chamber as it Appeared (a) Before Test and (b) After the Complete Burn of an Impact plate	12
5. Results of Particle Impact Tests on Impact Plates	13
6. Examples of the Results of Particle Impact Tests Using Rupture Disks	16
7. Results of Particle Impact Tests on Rupture Disks of Different Thicknesses	18
8. Heat Rate Per Unit Area Required for the Ignition of Monel 400, Stainless Steel 316, and Carbon Steel 1015 at Various Pressures	21
9. Frictional Heating Test Apparatus	23
10. Cross-Sectional Side View of Frictional Heating Test Chamber	24
11. Torque Load Measurement as Made (a) in Original Frictional Heating Apparatus and (b) in Test Apparatus as Modified for the Pressure Study and All Subsequent Tests	26
12. Representative Data from Frictional Heating Test 179 Conducted on Samples of Monel K-500 at 17000 rpm and 7 MPa	30
13. Examples of Results of Frictional Heating Tests	33
14. Pv Products Required to Ignite Pairs of Different Materials	45
15. Effects of Oxygen Pressure on the Sample Temperature and Coefficient of Friction for Monel K-500 (Test #236)	48
16. Effects of Oxygen Pressure on the Sample Temperature and Coefficient of Friction for Monel K-500 (Test #237)	49
17. Temperature of 1015 Carbon Steel When Frictionally Heated in $\text{GN}_2$ and Oxygen at 100, 1000, and 3000 psig	50

LIST OF FIGURES (Continued)

Figure		Page
A-1	Modified Particle Impact Chamber Used to Determine Temperature of Surface of Test Sample	A-1
A-2	Results of Tests to Determine the Temperature Difference Between the Test Sample Surface and the Test Chamber Inlet	A-2
B-1	Plummet Used in Dent-Comparison Test	B-1



## LIST OF TABLES

Table	Page
1. Summary of Pertinent Test Data for Pair of Like Materials	34
2. Average Heat Rate Per Unit Area (Pv Product) Required for Ignition by Frictional Heating of Pairs of Like Materials	36
3. Summary of Pertinent Test Data for Pairs of Different Materials	41
4. Average Heat Rate Per Unit Area (Pv Product) Required for Ignition by Frictional Heating of Pairs of Different Materials	43
5. Summary of Pertinent Data for the Effect of Oxygen Pressure on Frictional Ignition Materials	47
6. Ignition Temperatures of Carbon Steels and Monel Alloys Determined in Heated Bomb Tests	54
7. Sample Temperature and Pv Products Required for Ignition on a Function of Pressure	54

## 1.0 INTRODUCTION

In a continuing effort to develop a more economical Space Transport System (STS), the NASA Lewis Research Center (LeRC) has defined a series of propulsion goals (Cooper 1983) for a new generation of space-based Orbital Transfer Vehicles (OTVs). The propulsion system for the OTVs will use liquid hydrogen ( $LH_2$ ) and liquid oxygen ( $LO_2$ ) as propellants. The OTVs will be transported to one of several space stations using an STS Orbiter. Operating from a fueling station located near the space station, each of the OTVs will make up to 100 round-trip flights, transporting payloads to and from high orbits. Consequently, the OTV propulsion system must be able to use fuel more efficiently, have a longer life, and require less maintenance than the systems that are currently being used.

In an effort to meet these performance goals, Aerojet Liquid Rocket Company, under NASA Contract NAS 3-23772, has developed a new design concept for  $LH_2/LO_2$  engines. The design uses warm gaseous oxygen ( $GO_2$ ) at high pressure to drive the turbine in the  $LO_2$  turbopump. While this design concept eliminates several problems common to currently used engines, it creates new ignition hazards associated with the use of warm, high-pressure  $GO_2$ .

Two important ignition sources are present in rotating machinery such as the proposed  $LO_2$  turbopump. Ignition of the turbopump parts may be caused when heat is generated by mechanical rubbing due to thermal expansion or bearing failure. Ignition may also be caused when particles of foreign material entrained in the flow of  $GO_2$  or released at high velocity from the rotating turbine blade are impacted onto the surface of metal parts.

To determine the feasibility of the new turbopump design, the LeRC requested that selected materials be evaluated for their resistance to ignition in warm, high-pressure  $GO_2$ . LeRC requested that tests be conducted at the WSTF using several of the methods developed at WSTF to

determine the relative resistance to ignition of the materials. These methods consisted of an apparatus that expose materials to frictional heating and an apparatus that exposes materials to the impact of high-velocity particles.

A series of particle impact and frictional heating tests was conducted at WSTF. This report designated as volume I, will define the objectives of the test program, describe the test systems and procedures of the particle impact and frictional heating tests, and presents the test results. The raw data obtained from both the particle impact and the frictional heating tests are contained in appendices, designated as Volumes II through V.

## 2.0 OBJECTIVE

The overall objective of the program was to determine the relative resistance of nine selected materials to ignition when subjected to particle impact and frictional heating. To accomplish this overall objective, the program was divided into the following specific objectives: (1) To determine the resistance to ignition of the selected materials when exposed to or ruptured by the impact of particles entrained in a high-velocity oxygen stream at elevated temperatures and pressures. (2) To determine the resistance to ignition of the selected materials when pairs of like or different materials were rubbed together in gaseous oxygen at a constant pressure. (3) To determine the effects of varying oxygen pressure on the frictional heating of materials.

## 3.0 PARTICLE IMPACT TESTS

Particle impact tests were performed on targets configured as impact plates made of each of eight materials: Hastelloy X, Invar 36, Monel K-500, Monel 400, nickel 200, silicon carbide (SiC), stainless steel 316, and zirconium copper (Zi-Cu). Particle impact tests were also performed on targets configured as rupture disks made of type 316 stainless steel.

### 3.1 BACKGROUND

The initiation of fires in oxygen systems by the impact of high-velocity particles has been suspected for many years (Lapin 1972). Although the mechanism for ignition of metals by particle impact is not entirely understood, recent tests reported by Benz, Williams, and Armstrong (1985) have provided some insights.

The kinetic energy of impacting particles converted to heat after impact serves to ignite and burn the impacting particles. The heat produced from the burning particles serves to ignite the target materials. These two processes must occur in the short time period while the particles are in intimate contact with the target material. Thus, the rate of energy delivered to a specific cross-sectional area of the target material (energy flux density) by the burning particles is believed to be a critical parameter influencing the ignition phenomena.

When assessing the susceptibility of a system to ignition by particle impact, the following major factors must be addressed. First, information about the particles must be ascertained, such as the types and sizes of the particles. Then the environment that the particles will experience has to be addressed to determine if the particles contain sufficient kinetic energy to ignite. For example, at very high velocities (greater than 450 m/s) 1600  $\mu\text{m}$  aluminum particles ignite readily, whereas similar-sized particles of type 304 stainless steel do not ignite (Benz, Williams, Armstrong, 1985). And, as the size of the particles increases for a fixed velocity, the susceptibility of particles to ignition decreases (Thayer, 1971).

Once it has been determined that particles will ignite, the energy flux density produced by the burning particles must be assessed. For example, even though a small particle may ignite more easily, the number of particles may be small or the impact profile of the particles may be

large. In both cases a lowering of the energy flux density results. However, Nihart and Smith (1960) have shown that when a large number of small particles are present many materials can be ignited. As the size of the particles are increased, large energy flux densities can be achieved. However, the particles must ignite, and ignition of the particles becomes more difficult as the size of the particles are increased.

Finally, the ignition and burn characteristics of materials that will experience the impact of particles must be addressed. Materials which are very resistant to ignition or have low burn factors require high energy flux densities to ignite and burn, such as many small particles or a single large particle. In the case of a large particle, the size of the particle required to produced a sufficient energy flux density may be prohibitive for ignition of the particle under the dynamic conditions of the system.

### 3.2 TEST SYSTEM DESCRIPTION

The overall particle impact test system is shown schematically in Figure 1. The system consisted of a 15-m<sup>3</sup> (530-ft<sup>3</sup>) gaseous oxygen storage vessel, a remotely operated isolation valve and pressure regulator, a particle injection system, a heat exchanger, pressure and temperature measuring devices, and a test chamber. Gaseous oxygen was stored in a storage vessel at pressures up to 41.4 MPa (6000 psi). Flow of gaseous oxygen through the heat exchanger was controlled by the isolation valve and the pressure was set by means of the pressure regulator. The flowing oxygen, as it passed through the heat exchanger, was heated to temperatures ranging from 496 to 755 K (400 to 900°F). Particles were injected into the oxygen stream by establishing a slight push in the injector system.

Cross-sectional views of the test chamber are shown in Figure 2. Hot gaseous oxygen entered the test chamber through a test gas inlet port in the inlet adapter and was accelerated in an orifice. The hot oxygen then

entered into a plenum where it was accelerated to velocities greater than mach 2. Oxygen flow was then directed onto the target which was held in place with a retainer. The gaseous oxygen exited the chamber through three ports spaced at 120° intervals around the chamber.

The targets were configured as either impact plates or rupture disks (Figure 2). When the rupture disk configuration was used, a cup-shaped back-up plate was installed between the rupture disk and the retainer, forming a cavity behind the disk. Three small holes in the rupture disk allowed the gaseous oxygen to flow into the cavity, thus equalizing the pressure on both sides of the disk.

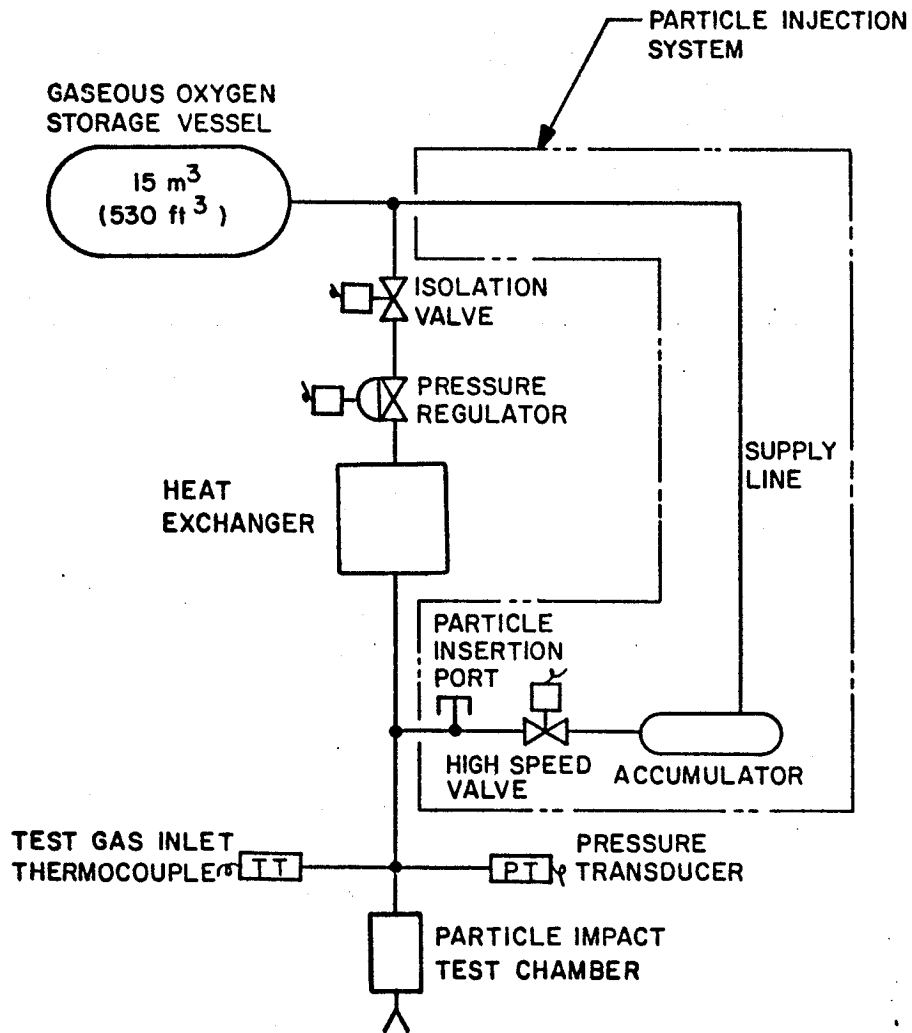
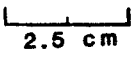


Figure 1: Schematic Diagram of the Gaseous Oxygen Test System with the Particle Impact Chamber Installed

SCALE:   
2.5 cm  
(1 INCH)

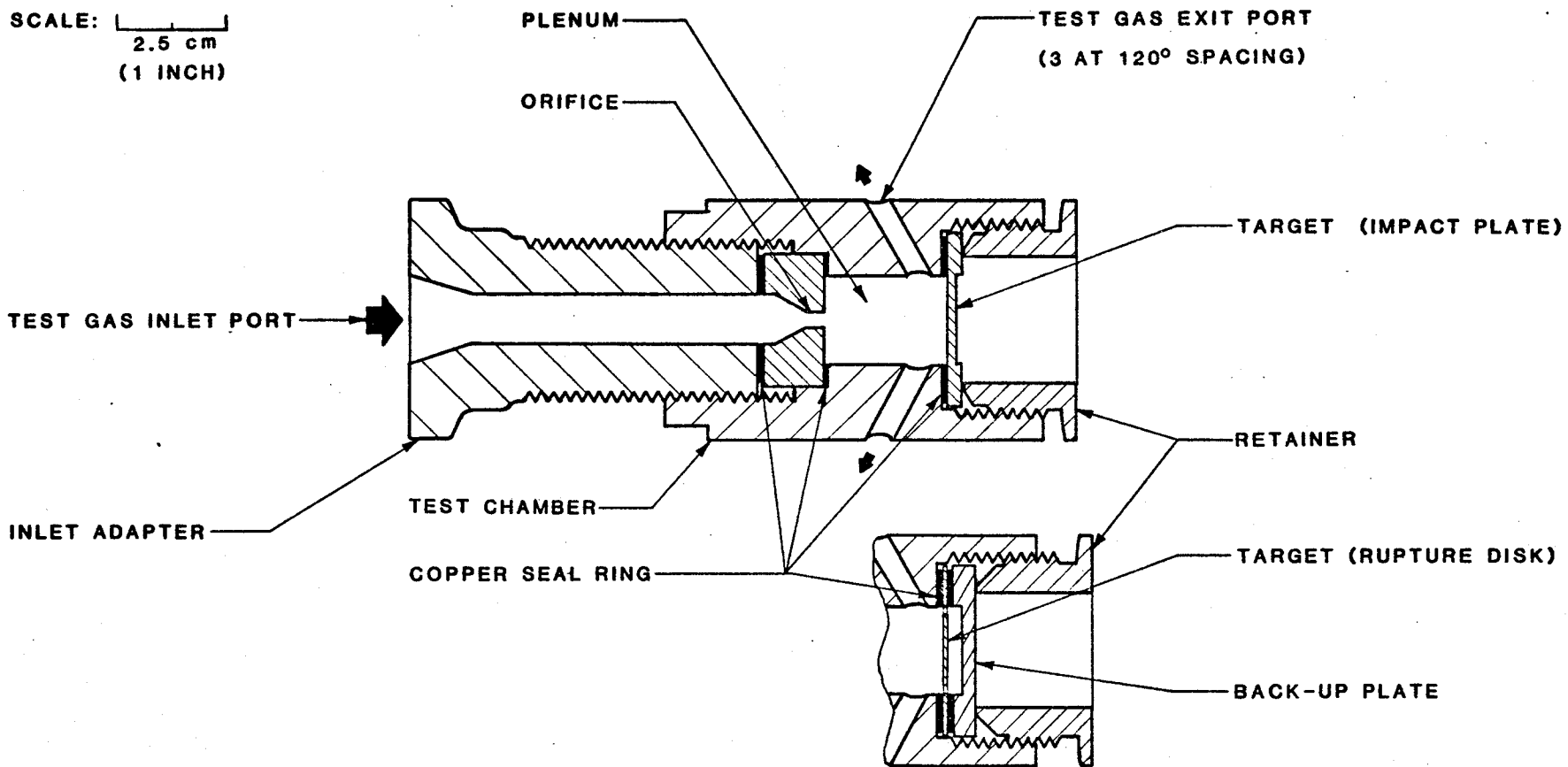


Figure 2: Cross-Sectional View of the Particle Impact Test Chamber Showing Two Target Configurations

The temperature and pressure of the oxygen were measured at the inlet to the test chamber using a Type K thermocouple and a bonded strain-gauge pressure transducer. All instrumentation was connected to a data acquisition system which processed and recorded the data. Calibration tests were performed to determine the differences between the inlet oxygen temperature and the target surface temperature, see Appendix A. The results indicated that the target surface temperature was 22 to 39 K (40 to 70°F) higher than the oxygen inlet temperature. Calibration tests were also performed to determine the velocity of the particles which were injected into the oxygen stream, see Appendix B, and indicated that the minimum velocity of the particles were approximately 260 m/s (853 ft/s).

### 3.3 TEST CONSIDERATIONS

In these tests, the objective was to determine the relative resistance of materials to ignition when exposed to particle impact -- not the resistance of the particles to ignition. Therefore, the type and size of particles were selected based on their ease to ignite and the quantity of heat released during combustion. Aluminum particles were selected for this test because previous experience at WSTF has indicated that aluminum particles with diameters of greater than 1600  $\mu\text{m}$  could be ignited at the conditions produced in the particle impact test chamber. Assuming that the impact area was proportional to the diameter of the particle, the energy released from burning one 1580  $\mu\text{m}$  (0.063 in) diameter spherical aluminum particle was 0.118 kJ for an impact area of 0.020  $\text{cm}^2$ . This energy release for aluminum was greater than or equal to the energy release for other materials with the exception of beryllium. Therefore, aluminum particles were considered to represent the worst case ignition source for particle impact testing.

At least five impact tests, using new target materials, were conducted on each material configured as impact plates. In each test, the target material was subjected to ten 1580  $\mu\text{m}$  diameter particles made of aluminum 2017-T4 which represented a total energy release of 1.18 kJ, randomly distributed across the target material surface (2.85  $\text{cm}^2$ ). In addition



a series of 10 tests was conducted with a nickel 200 target without replacing the target between tests.

A series of tests was conducted to determine whether target samples that rupture upon impact were more or less likely to ignite than target samples that did not rupture upon impact. The target samples consisted of type 316 stainless steel disks designed to rupture upon impact by aluminum particles. Nine tests were conducted on rupture disks 0.5 mm (0.020 in) thick, and five tests were conducted on rupture disks 0.4 mm (0.015 in) thick.

The relative resistance to ignition of the selected materials was determined by varying the inlet oxygen temperature, which, in turn, varied the surface temperature of the materials. Materials that required relatively higher temperatures for ignition were assumed to be more resistant to ignition by particle impact than materials that ignited at lower temperatures.

### 3.3.1 SAMPLE PREPARATION

Target materials configured as impact plates were machined from stock materials to a thickness of 0.15 cm (0.060 in). These impact plates allowed for a cross-sectional area of 2.85 cm<sup>2</sup> (0.44 in<sup>2</sup>) exposed to the impacting particles. Target materials configured as rupture disks were cut from sheet materials, 0.38 and 0.5 mm (0.015 and 0.020 in) thick, allowing for a cross-sectional area of 2.85 cm<sup>2</sup> to be exposed to the impacting particles.

All target materials were cleaned by washing them with a sodium hydroxide solution, then with a phosphoric acid solution, and finally with an emulsion agent. The materials were rinsed with isopropyl alcohol and then with Freon 113. The materials were then dried with nitrogen and individually sealed in Teflon bags.

### 3.3.2 TEST CONDITIONS

In each test, 10 spherical particles, 1580  $\mu\text{m}$  (0.063 in) in diameter, were injected into a heated stream of oxygen at the inlet to the chamber. The oxygen stream was maintained at a mass flow rate of 0.45 kg/s (1 lbm/s), a pressure of 31.5  $\pm$  1.2 MPa (4575  $\pm$  175 psig), and temperatures between 496 and 755 K (400° and 900° F). The particles entrained in the oxygen stream were accelerated to a velocity of approximately 260 m/s (860 ft/s). The average oxygen pressure in the plenum was approximately 4.1  $\pm$  0.7 MPa (600  $\pm$  100 psig). The target surface temperature was 22 to 39 K (40 to 70°F) hotter than the temperature of the gaseous oxygen at the inlet to the test chamber. The velocity of the particles was greater than 262 m/s (861 ft/s).

### 3.3.3 TEST PROCEDURE

In each test, the target material was installed into the test chamber and the retainer was tightened. The particles were placed in the particle insertion port and sealed. The accumulator was pressurized to the maximum pressure available in the storage vessel, which was at least 2.8 MPa (400 psig) above the test pressure. After the test area was cleared of all personnel, the pressure regulator was adjusted and the flow of oxygen was initiated by opening an isolation valve. The data acquisition system was activated to monitor and record temperature and pressure at the inlet to the test chamber once every 100 ms during the test. When the desired test conditions were achieved, the particle injection high-speed valve was opened briefly and then closed, thereby injecting the particles into the flowing oxygen stream. Two seconds after the particles were injected, the isolation valve was closed and the flow of oxygen was stopped. The target was then removed and examined for evidence of burning. In the series of 10 particle impact tests performed using the same nickel 200 impact plate, the impact plate was examined after each test and then replaced in the test chamber.

## 3.4 PARTICLE IMPACT RESULTS

### 3.4.1 Test With Impact Plates

The following sections summarize the results of tests in which impact plates were used as targets. Appendix C contains complete test results for each individual test.

#### 3.4.1.1 Types of Ignition Event Observed

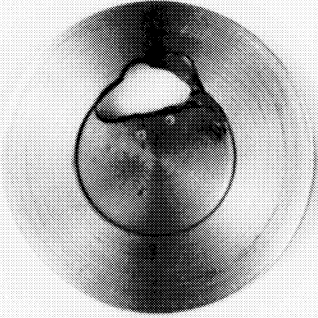
When subjected to particle impact, the impact plates either did not burn, showed slight burning on the target surface, burned partially, or burned completely (Figures 3 and 4). The results of a test in which a zirconium copper sample did not ignite upon particle impact are shown in Figure 3a. The dents made in the sample by the impacting particles can be seen in the photograph. Similar dents typically appeared on impact plates that did not ignite upon impact.

The results of a test in which a Hastelloy X sample exhibited only slight surface burning upon particle impact are shown in Figure 3b. A small triangle-shaped marking extends from the center of a dent made by an impacting particle. Careful observation of the mark reveals that some of the material has been removed from the surface of the impact plate by erosion or burning.

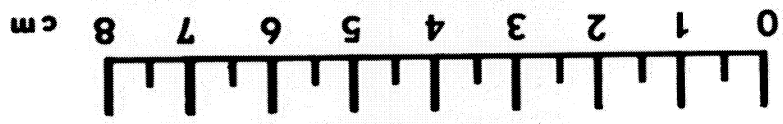
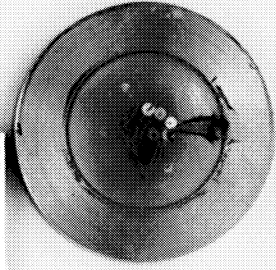
The results of a test in which a type 316 stainless steel sample partially burned are shown in Figure 3a. A hole extending through the target material is visible and indicates that partial combustion of the test material occurred. Burning quenched before the entire target material was consumed. Each of the impact plates that burned partially exhibited a similar burn pattern.

The results of a test in which a type 316 stainless steel target material burned completely are shown in Figure 4. Figure 4(b) shows the end view

(c)  
STAINLESS STEEL 316 IMPACT PLATE  
- PARTIAL BURN -



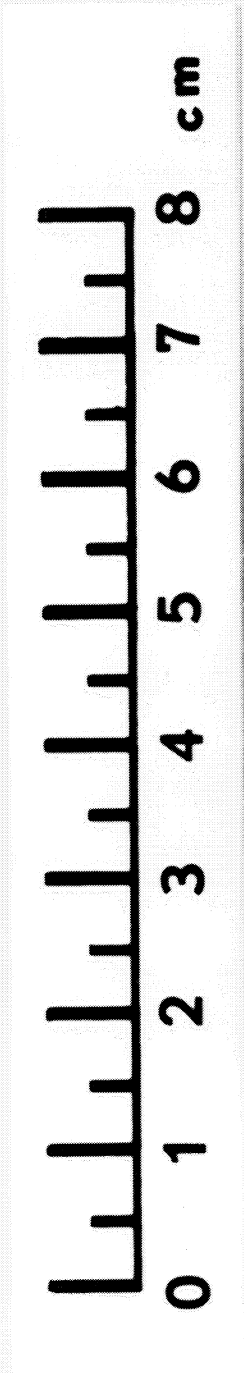
(b)  
HASTELLOY X IMPACT PLATE  
- SLIGHT EVIDENCE OF BURNING -



(a)  
ZIRCONIUM COPPER IMPACT PLATE  
- NO BURNING -



Figure 3:  
Impact Plates Showing (a)  
No Burning, (b) Slight  
Evidence of Burning, (c)  
Partial Burning



BEFORE TEST

AFTER TEST

Figure 4: End View of a Test Chamber as it Appeared (a) Before Test and (b) After the Complete Burn of an Impact Plate

ORIGINAL PAGE  
BLACK AND WHITE PHOTOGRAPH

of an assembled test chamber after a type 316 stainless steel target burned completely. The target material, the back of which can be seen in the photograph of the pretest assembly, was completely consumed by the reaction. The retainer was almost completely destroyed and the test chamber was irreparably damaged. Such extensive damage to the test chamber was typical of the tests in which target materials were totally consumed.

### 3.4.1.2 Ignition Susceptibility of the Materials

The ignition events resulting from the tests in which target material were configured as impact plates are shown as a function of the initial oxygen temperature in Figure 5. Complete burning occurred only with samples of Invar 36 and type 316 stainless steel. In tests with Invar 36, the sample burned completely in 6 out of 12 tests conducted at oxygen temperatures above 625 K (655 °F). The frequency with which the

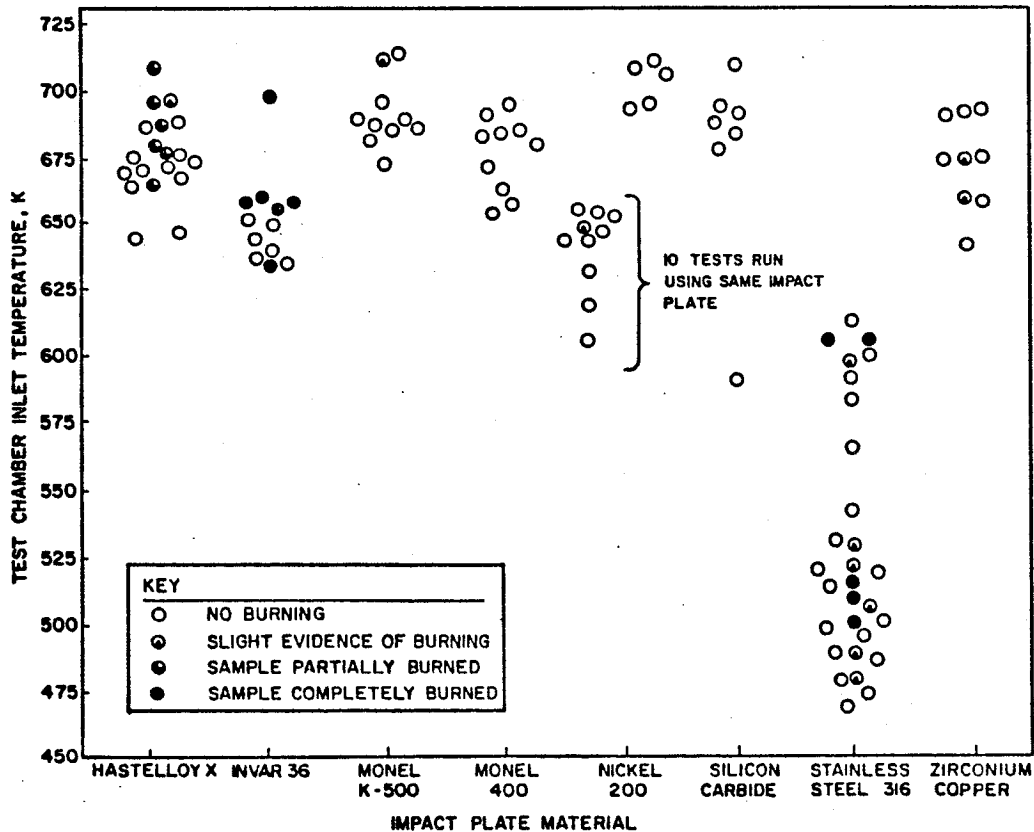


Figure 5: Results of Particle Impact Tests on Impact Plates

Invar 35 burned completely appeared to increase as the oxygen temperature increased. In the 29 tests conducted with type 316 stainless steel at oxygen temperatures between 450 and 625 K (350 and 665 °F), five tests resulted in complete burning of the target, and six tests resulted in only slight surface burning of the target. The frequency with which any types of burning occurred was not apparent to be a function of the oxygen temperature for type 316 stainless steel.

When targets of Hastelloy X were tested, partial burning occurred in 6 of the 19 tests conducted at oxygen temperatures above 625 K (665 °F), and slight surface burning was observed in one other test. The frequency of the burning events appeared to increase as the oxygen temperature was increased.

Samples of the remaining target materials either did not burn or showed slight surface burning at oxygen temperatures above 625 K (665 °F). Monel 400 and silicon carbide showed no evidence of burning. Monel K-500 and zirconium copper showed slight surface burning, as did nickel 200 in one test. However, this one test with nickel 200 that produced slight surface burning was the ninth test in a series of ten tests using the same nickel 200 target as the impact plate. The burning event may have been initiated from a particle impacting on aluminum deposited on the surface of the target in the previous eight tests. When nickel 200 targets were replaced after each test, no evidence of burning was observed out of five tests at oxygen temperatures above 675 K (755 °F).

#### 3.4.1.3 Discussion of Test Results

The objective of these tests was to determine the relative resistance of selected materials to ignition by particle impact. In a broad sense, Monel 400, silicon carbide, and nickel 200, can be ranked as the materials most resistant to ignition, since no samples of these materials were observed to burn in the limited number of tests

performed. Similarly, type 316 stainless steel and Invar 36 can be ranked as the materials least resistant to ignition, since samples of these materials were observed to burn completely.

However, an absolute rating for the remaining three materials, which exhibited partial or slight surface burning, is difficult to determine. In general, Hastelloy X, which exhibited partial burning, can be ranked as less resistant to ignition than Monel K-500 and zirconium copper, which exhibited only slight evidence of burning.

Efforts were made to further rank type stainless steel 316 and Invar 36, the materials that exhibited common burn types, by comparing the frequencies of ignition as a function of oxygen temperature. Statistical analysis of the test data using the Probit Method (Natrella 1963) indicated only that a larger number of data points was required for analysis because of what appeared to be a randomness of the ignition events as a function of temperature.

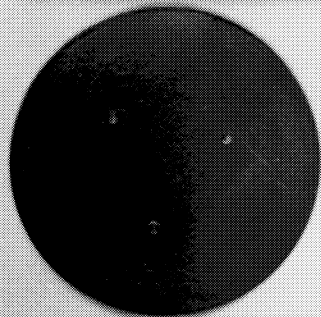
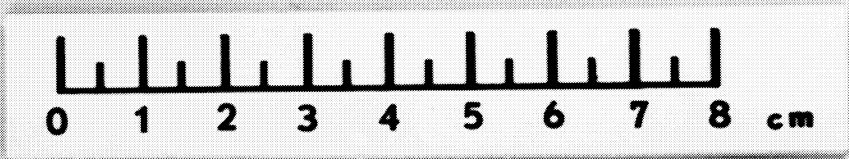
#### 3.4.2 Test With Rupture Disks

The following sections summarize the results of tests in which rupture disks made of type 316 stainless steel were used as targets. Appendix C contains complete test results for each of the individual tests.

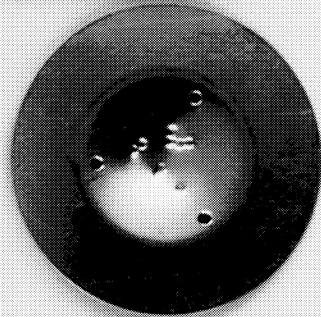
##### 3.4.2.1 Types of Ignition Events Observed

When subjected to particle impact, the target materials configured as rupture disks neither ruptured nor burn, ruptured but did not burn, or both ruptured and burned completely (Figure 6). A rupture disk as it appeared prior to test is shown in Figure 6a. The result from a particle impact test in which a disk neither ruptured nor burned is shown in Figure 6b. Dents caused by the impact of the particles are visible. Similar dents appeared on disks that neither ruptured nor burned upon impact.

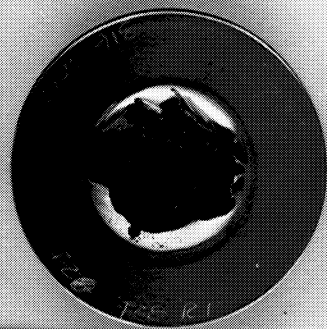




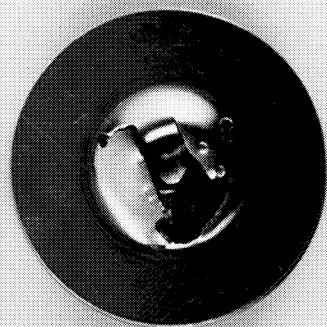
(a)  
RUPTURE DISK BEFORE TEST



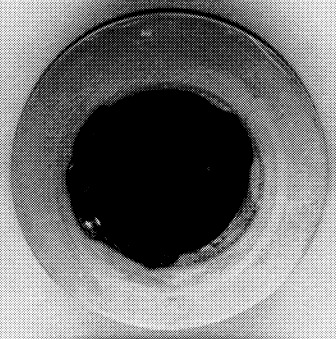
(b)  
NO RUPTURE, NO BURNING



(d)  
RUPTURE PRIOR TO PARTICLE IMPACT  
NO BURNING



(c)  
RUPTURE DUE TO PARTICLE IMPACT  
NO BURNING



(e)  
BURNED RUPTURE DISK

Figure 6: Examples of the Results of Particle Impact Tests Using Rupture Disks

NASA-WSTIF  
100E 10002

The result of a test in which a disk was ruptured by the particles but did not burn is shown in Figure 6c. The dents made in the disk by the particles are visible. In some of the tests at the lower inlet gas temperatures, dents appeared on the rupture disk but not on the back-up plate behind the disk, indicating that the disk was hit and ruptured by the particles. In tests at higher inlet gas temperatures, dents appeared on both the disk and back-up plate, indicating that the first particles to arrive hit and ruptured the disk, and the following particles hit and dented the backup plate.

A disk that was ruptured prior to impact by particles is shown in Figure 6d. No evidence exists that a particle hit the disk, although several dents can be seen on the backup plate. A rupture disk that was burned is shown in Figure 6e. The material in the impact area was consumed and the fire was quenched at the inside edge of the copper seal ring.

#### 3.4.2.2 Ignition Resistance of the Material

Of the five target materials configured as rupture disks that were 0.38 mm (0.015 in) thick, two neither ruptured nor burned and three ruptured but did not burn (Figure 7). When the temperature of the inlet gas was increased above 513 K (465 °F), the disk was ruptured prior to the impact of particles. Of the rupture disks that were 0.5 mm (0.020 in) thick, two neither ruptured and nor burned, three ruptured but did not burn, and four ruptured and burned completely. Generally, the disks ruptured and burned more frequently at the higher temperatures. In one case, the disk burned at only 489 K (420 °F), which was more than 28 K (50 °F) lower than the temperature at which two disks neither ruptured nor burned. However, it is uncertain if the disk ruptured and then burned, or if the disk did not rupture but ignited and burned by only particle impacts. Included in Figure 7 are the results for the type 316 stainless steel target materials configured as impact plates.

### 3.4.2.3 Discussion

The results of the limited testing conducted with rupture disks did not provide enough information to determine whether materials configured as rupture disks were more likely to ignite upon particle impact than materials configured as impact plates. Therefore, the process of rupturing and its effects on the ignition of target materials could not be discerned. A large number of additional tests would have been required to make this determination but was prohibited because of the lack of funds available.

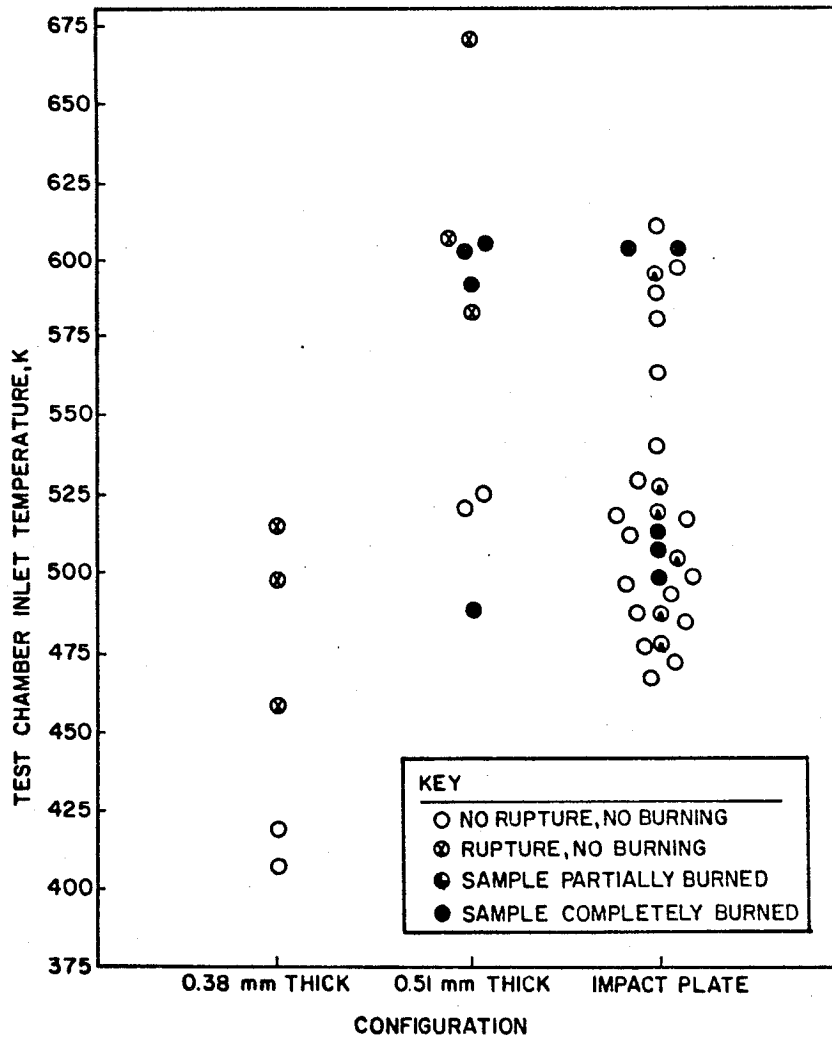


Figure 7. Results of Particle Impact Tests on Rupture Disks of Different Thickness

#### 4.0 FRICTIONAL HEATING TESTS

Frictional heating tests were performed at the same oxygen pressure on test samples made of pairs of like materials. The following nine materials were evaluated: Hastelloy X, Inconel 600, Invar 36, Monel K-500, Monel 400, nickel 200, silicon carbide (SiC), stainless steel 316, and zirconium copper (Zi-Cu). Frictional heating tests were then performed on pairs of test samples made from different materials in which stationary and rotary test specimens were fabricated from the following materials:

<u>Rotary Sample</u> <u>Materials</u>	<u>Stationary Sample</u> <u>Materials</u>
Monel K-500	Nickel, Electra-Formed (ED)
Silicon Carbide (SiC)	Invar 36
Silicon Carbide (SiC)	Monel K-500
Stainless Steel 316	Monel K-500
Stainless Steel 316	Zirconium Copper (Zi-Cu)

Finally, an attempt was made to determine the effect of oxygen pressure on the ignition of the materials when they were subjected to frictional heating. The test samples were made of Monel K-500.

#### 4.1 BACKGROUND

Heat produced when two materials are rubbed together has been suspected for many years as being the cause of oxygen-metals fires in turbopumps (Naegeli 1971; Clark and Hust 1974). The frictional energy produced from the rubbing process can be described by the following relationships:

$$Q_f = \omega L = P v A \mu \quad (1)$$

where A: cross sectional area (m<sup>2</sup>)  
P: contact pressure (N/m<sup>2</sup>)

- L: torque (Nm)
- v: average linear surface velocity (m/s)
- $\omega$ : angular velocity (radian/s)
- $\mu$ : coefficient of friction

By rearranging Equation 1, a power term can be obtained represented by the product of the contact pressure (P) and average linear surface velocity (v), Equation 2.

$$Pv = \frac{L\omega}{A\mu} \quad (2)$$

The units of Pv product reduce to W/m<sup>2</sup> but are more conveniently expressed as N/m<sup>2</sup>-m/s or lbf/in<sup>2</sup>-in/min. The Pv product required for ignition provides a means for comparing the relative resistance of materials to ignition. Materials requiring large Pv products for ignition are more resistant to ignition than materials requiring small Pv products.

Frictional heating tests are highly dependent on the physical properties of the material. The heat required to ignite a material by frictional heating is dependent on the coefficient of friction which is dependent on the surface properties, hardness, compressive strength, and temperature of the material. Therefore, besides evaluating the resistance of materials to ignition, the frictional heating test also evaluates the heat generating properties of the materials during the rubbing process.

Heat generated from a rubbing process occurs in seconds, which is a long period of time, as compared to milliseconds in the particle impact test. Thus, mechanisms for heat transfer can play a major role in affecting the Pv product required to ignite a particular material. For example, Benz and Stoltzfus (1985) reported that varying oxygen pressure or rotational speed could vary the convective heat transfer from materials which was shown to affect the Pv products required for ignition. The effects of varying oxygen pressure on the Pv products required for ignition are

shown in Figure 8. The increase in the Pv product as oxygen pressure was increased above 1 MPa (145 psia) was attributed to convective cooling caused by the increase in the oxygen density around the samples. Below 1 MPa oxygen, the Pv products were observed to increase as pressure was decreased, which was attributed to reduced oxidation rates. It was this pressure effect on the Pv products required for ignition that generated the requirement for the pressure study conducted in this program.

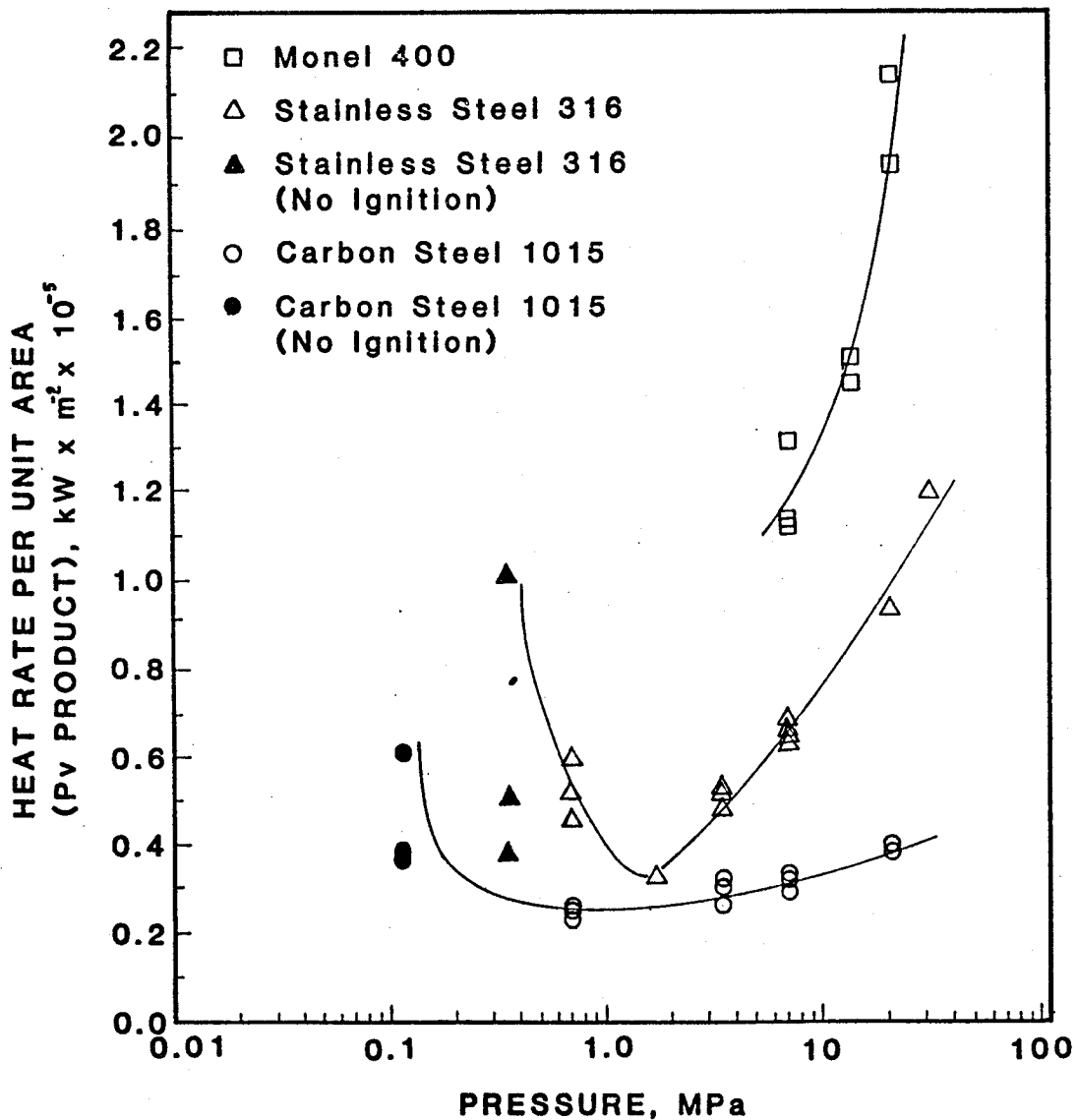


Figure 8: Heat Rate Per Unit Area Required for the Ignition of Monel 400, Stainless Steel 316, and Carbon Steel 1015 at Various Pressures (From Benz and Stoltzfus 1985)

## 4.2 TEST SYSTEM DESCRIPTION

The basic WSTF frictional heating apparatus was used for all tests for this portion of the test program. A modification of the apparatus was made during the course of this program to support the requirement for a more accurate torque measurement.

The frictional heating apparatus (Figure 9) consisted of a high pressure test chamber, an electrical motor and transmission assembly, and a pneumatic actuation cylinder. The high pressure test chamber (Figure 10) consisted of a cylindrical chamber with an outside diameter of 12.7 cm (5 in) and an inside diameter of 3.8 cm (1.5 in) and fabricated from Monel 400. The internal cavity of the chamber was provided with a replaceable copper sleeve and had a volume of 49 cm<sup>3</sup> (3 in<sup>3</sup>). The chamber contained a rotating shaft that extended through the chamber attached at one end to the drive motor-transmission assembly and at the other end to the pneumatic actuation cylinder. The drive motor-transmission assembly consisted of 15 H.P., constant speed electric motor and a variable speed belt driven transmission. The assembly provided the capability to rotate the shaft at rotational speeds over a range from 3,000 and 17,000 rpm. The pneumatic actuation cylinder consisted of a cylinder pressurized with nitrogen and actuation linkage that provided for axial movement of the shaft and for the capability to apply normal loads of up to 3160 N (710 lbf) on the test samples.

Identical housings containing bearings and seals were attached to both ends of the chamber. Sealing the chamber for high pressure oxygen was accomplished in these housings by mounting two seals on the rotating shaft in each housing on either side of a copper cooling block. The copper cooling block was provided with flowing water under high pressure to cool the seals and to provided a back pressure to the chamber pressure seals.

The test sample consisted of two identical hollow cylinders, with outside diameters of 2.5 cm (1 in) and inside diameters of 2.0 cm (0.8 in).

These test samples provided a rubbing surface of 1.8 cm<sup>2</sup> (0.28 in<sup>2</sup>). One sample was mounted to the rotating shaft and the sample was affixed to the chamber via a sample mounting housing. Contact of the two samples was accomplished by pulling the shaft and rotating sample against the fixed sample using the pneumatic actuation assembly. In the original design, the sample housing was attached directly to the chamber such that as the samples rubbed, torque was applied to the entire chamber. Movement of the chamber was restrained by an extended arm, attached to the chamber at one end, and positioned against a load cell at the other end (Figure 11a). This design was the original method for measuring torque produced by the rubbing samples.

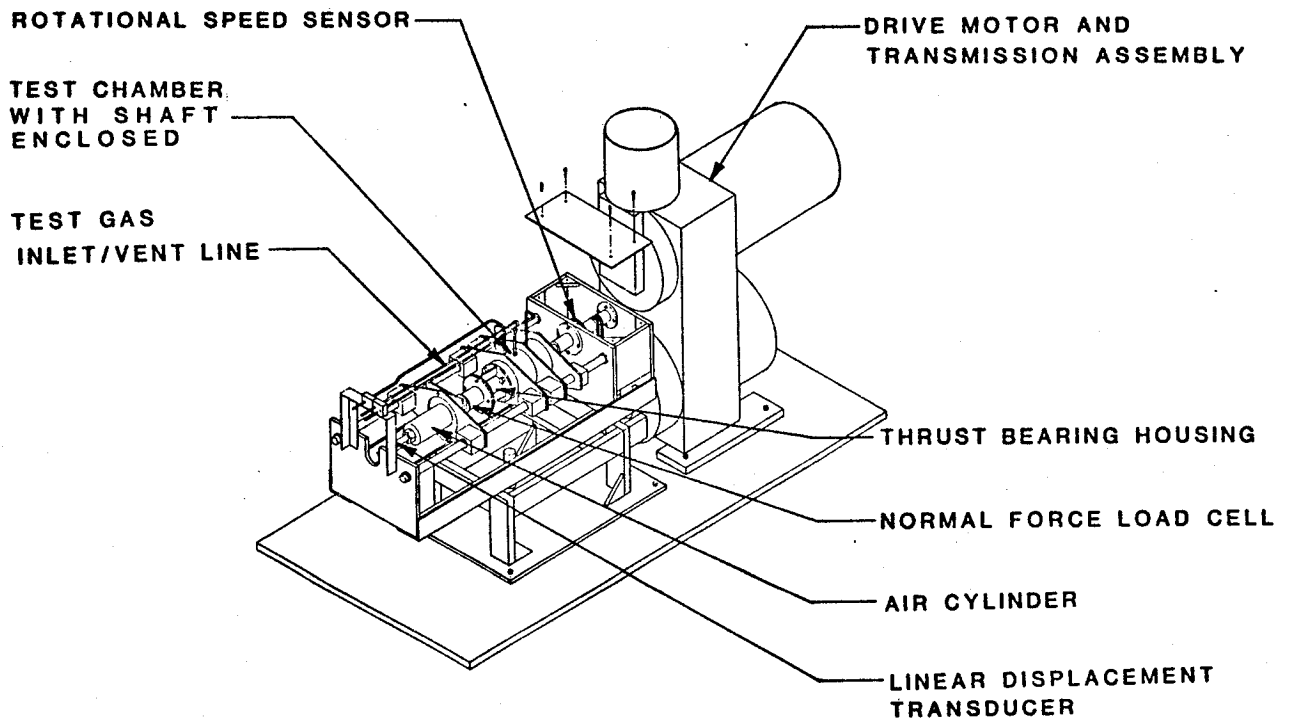


Figure 9: Frictional Heating Test Apparatus



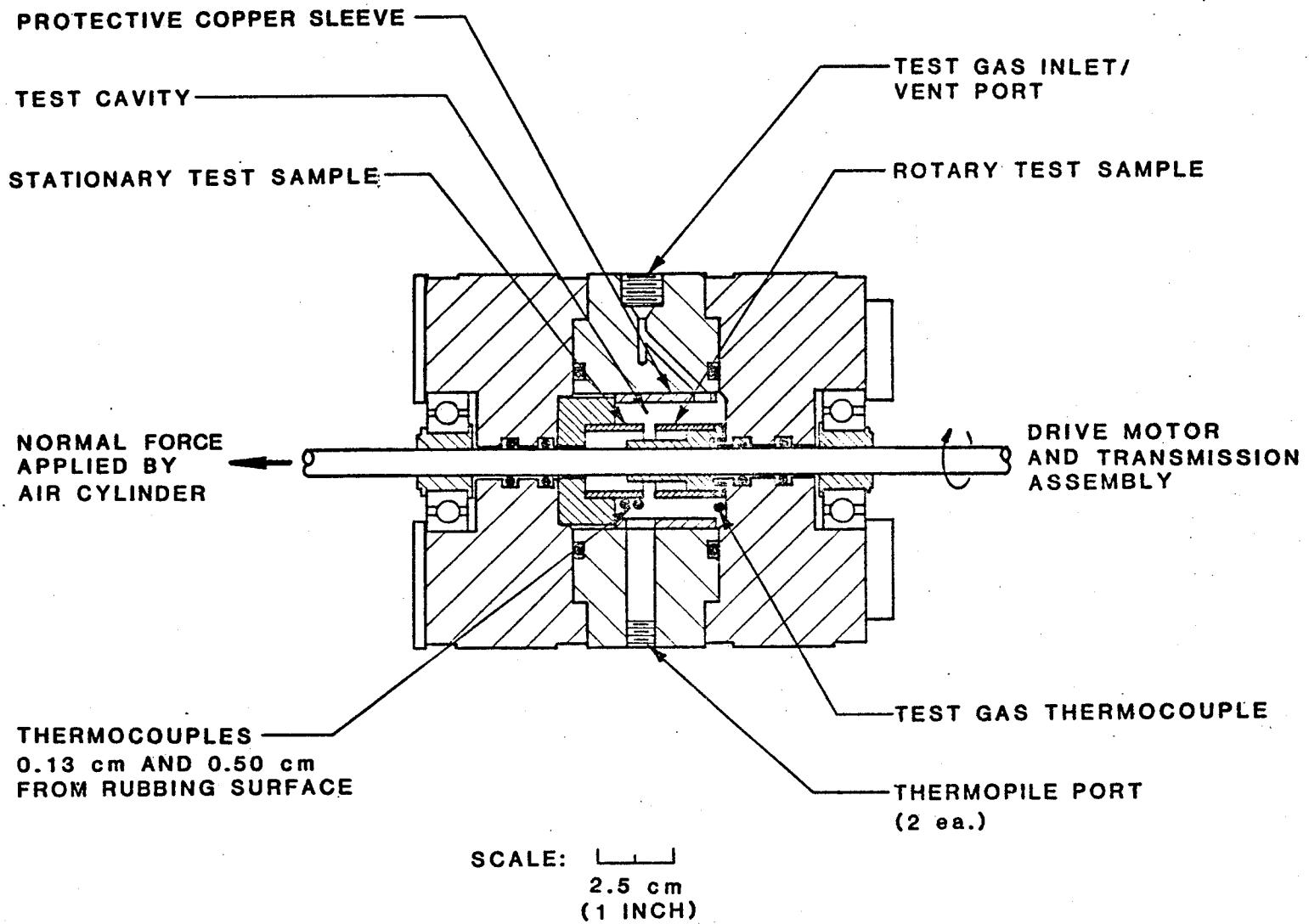


Figure 10: Cross-Sectional Side View of Frictional Heating Test Chamber

During the course of the program, a more accurate torque measurement was required to support testing to determine the effect of varying oxygen pressure on frictional heating of the test samples. The method for measuring torque was changed by mounting the sample housing in a bearing which was attached to the chamber. Movement of the sample housing was restrained by a pin positioned against a load cell (Figure 11b).

Oxygen and nitrogen was provided to the chamber via a high pressure gas distribution system which was interfaced to the WSTF High Pressure Oxygen Test Facility. The system was capable of providing and regulating oxygen up to 68.9 MPa (10,000 psia) and nitrogen up to 20.7 MPa (3,000 psia).

Instrumentation consisted of the following: Pressure in the chamber was measured using a 0 to  $68.9 \pm 0.7$  MPa (12 to  $10,000 \pm 100$  psia) digital Bourdon tube gauge and pressure in the pneumatic actuation cylinder was measured using a 0 to  $6.9 \pm 0.07$  MPa (0 to  $1000 \pm 10$  psia) bonded strain gauge transducer. Temperature of the oxygen and the fixed test sample, 0.13 and 0.51 cm (0.05 and 0.20 in) from the rubbing surface, were measured using sheathed Chromel-Alumel thermocouples with accuracies of  $\pm 1$  K (2 °F). The temperature of the rubbing surface above 1200 K (1700 °F) was measured using a two-color optical pyrometer. Normal load applied to the samples was measured using a 0 to  $4450 \pm 22$  N (0 to  $1000 \pm 10$  lbf) load cell, and torque from the rubbing samples was measured using 0 to  $890 \pm 5$  N (0 to  $200 \pm 2$  lbs) load cell. Axial displacement of the rotating shaft or sample wear was measured using a linear displacement transducer with an accuracy of 0.013 cm (0.005 in). Rotational speed of the shaft was measured using a 0-20,000 rpm sensor with an accuracy of  $\pm 3$  percent of full speed.

The data were digitally processed by a microprocessor and stored on a floppy disk. Data from each instrumentation channel were stored every 100 ms and represented an average value of eight readings taken 8 ms prior to the stored value.

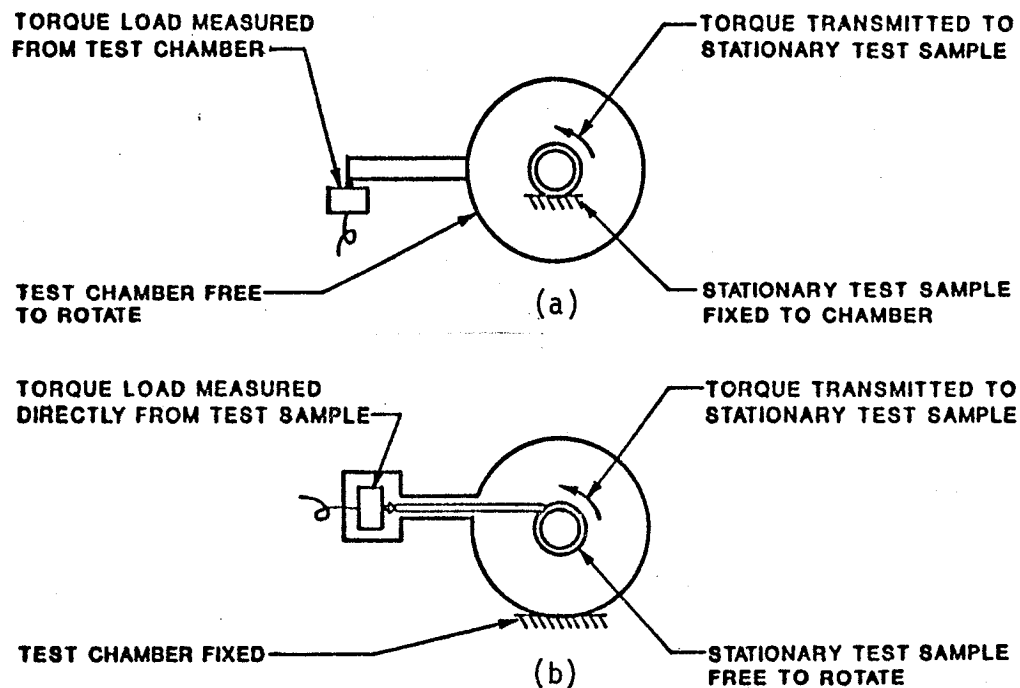


Figure 11: Torque Load Measurement as Made (a) in Original Frictional Heating Apparatus and (b) in Test Apparatus as Modified for the Pressure Study and All Subsequent Tests

#### 4.3 TEST CONSIDERATIONS

One of the objectives of these tests was to determine the relative resistance to ignition of selected materials when pairs of the same or different materials were rubbed together. The test logic used to accomplish this task, consisted of measuring and then comparing the products of the contact pressure ( $P$ ) and linear surface speed ( $v$ ) or  $Pv$  product required for ignition. The  $Pv$  products were determined by holding the surface speed constant while increasing the contact pressure on the samples at a fixed rate until ignition of the samples occurred. The value of the contact pressure at the point of ignition was used to calculate the  $Pv$  product. Ignition of the materials was defined as an event that produced a rapid increase in the sample temperature, rapid release of radiant energy, and rapid sample consumption. Ignition was verified by posttest visual examination of the samples. At least three tests with new sample pairs were conducted on each material.

Another objective of these tests was to determine the cause for the increased in the  $Pv$  product required for ignition as oxygen pressure was

increased (Benz and Stoltzfus 1985), as discussed in Section 4.1. It was postulated that the cause was a decrease in the coefficient of friction, an increase in convective cooling as oxygen pressure was increased, or both. In both cases the temperature of the sample should decrease as pressure is increased for a fixed Py product. The test logic consisted of rubbing a pair of materials at a constant contact pressure and surface velocity initially at some low oxygen pressure until temperature equilibrium of the samples was achieved. The oxygen pressure was then increased to a new value without changing the contact pressure or surface velocity until temperature equilibrium of samples was again achieved. Three oxygen pressures per test were evaluated. The relative changes in the coefficient of friction and sample temperatures as a function of oxygen pressure were measured and compared.

#### 4.3.1 Sample Preparation

The test samples were machined from stock material into hollow cylinders with outside diameters of 2.5 cm (1 in) and inside diameters of 2.0 cm (0.8 in) and 2.2 cm (0.88 in) long. The samples were then washed with a sodium hydroxide solution, then with a phosphoric acid solution, and, finally, with an emulsion agent. The samples were rinsed with isopropyl alcohol and then Freon 113. The samples were dried with nitrogen and sealed individually in Teflon bags.

#### 4.3.2 Test Conditions

The following conditions were used to conduct tests to determine the relative ignition resistance on pairs of like and different materials. Oxygen test pressure was set at  $6.9 \pm 1$  MPa ( $1000 \pm$  psig) and at ambient initial temperature. The rotary test sample was turned at a rate of 17,000  $\pm$  200 rpm, resulting in a linear surface velocity of  $20.3 \pm 0.2$  m/s ( $67.8 \pm 8$  ft/s). The normal force applied to the test samples was increased from 0 to 3160 N (0 to 710 lbf) at a rate of 31 N/s (7.0 lbf/s). This normal force resulted in an increase in the contact pressure, normal force divided

by the cross-sectional area of the test sample, from 0 to  $17.3 \times 10^6$  N/m<sup>2</sup> (0 to 2500 lbf/in<sup>2</sup>) at a rate of  $1.7 \times 10^5$  N/m<sup>2</sup>/s (24 lbf/in<sup>2</sup>/s).

The following conditions were used to conduct tests to determine the effect of increasing oxygen pressure on the ignition of materials by frictional heating. The rotary sample was turned at a rate of 5000 rpm, resulting in a linear surface velocity of 6 m/s (19.6 ft/s). The normal force applied on the samples was held constant at approximately 378 N (85 lbf) or a contact pressure of  $2.1 \times 10^6$  N/m<sup>2</sup> (300 lbf/in<sup>2</sup>) without changing surface velocity or contact pressure. Oxygen pressure was increased from 0.69 MPa (100 psia) to 6.9 MPa (1000 psia) and, finally, to 20.7 MPa (3000 psia). The samples were rubbed long enough at the particular oxygen pressure to achieve temperature equilibrium.

#### 4.3.3 Test Procedure

In each test, the samples were mounted in the test chamber, and the test area was cleared. The test chamber was pressurized with oxygen to 6.9 MPa (1000 psig) and vented. This pressurization/venting cycle was repeated three times to ensure that air was purged from the test chamber. The test chamber was pressurized to the desired test oxygen pressure and then isolated from the oxygen source. The drive motor was then turned on and the desired rotational speed was established.

After the initial test conditions were obtained, the data acquisition system was activated. The test was initiated by pressurizing the pneumatic actuation cylinder which applied the desired normal force or contact pressure between the rotary and stationary samples. In tests where the relative ignition resistance of pairs of like and different materials were determined, the pneumatic actuation cylinder was pressurized at a steady rate until either ignition of the samples occurred or the maximum capability of the system was reached.

In tests where the effects of oxygen pressure on the ignition of materials were determined, the pneumatic actuation cylinder was

pressurized rapidly to a value that equated to the normal force or contact pressure desired between the test samples. The samples were rubbed until temperature equilibrium was achieved, at which time the oxygen pressure in the chamber was increased without changing the contact pressure or surface velocity.

After the test was completed, the data acquisition system was turned off, the test chamber was vented, and the test samples were removed and visually examined.

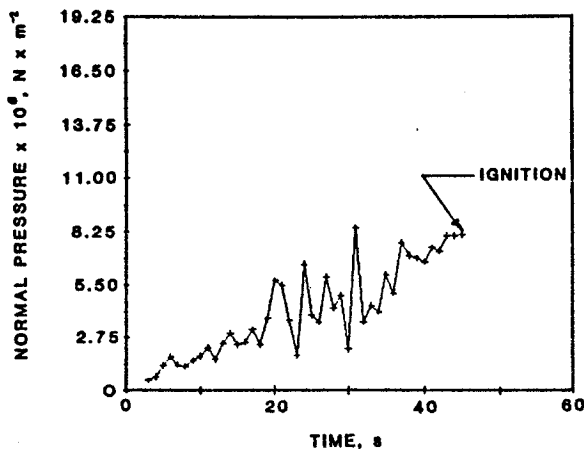
#### 4.4 FRICTIONAL HEATING TEST RESULTS

The following sections summarize the results for tests conducted to determine the relative ignition resistance of pairs of like and different materials, and the effects of oxygen pressure on the ignition characteristics of materials. Appendixes D-F contains complete test results for each of the individual tests conducted.

##### 4.4.1 Ignition Resistance of Pairs of Like Material

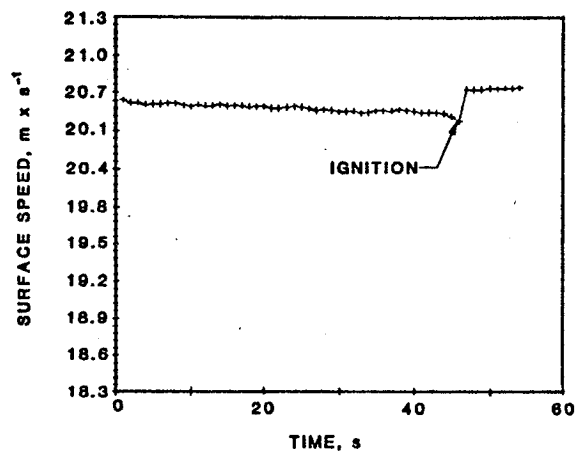
###### 4.4.1.1 General Comments Concerning the Data

Typical data obtained for each test run are shown in Figure 12 for Monel K-500 and illustrates the typical test parameters that were monitored during a test run. The primary use of these data was to determine the point of ignition and the Pv product required for ignition of the test materials. For example, ignition of Monel K-500 in this test run is clearly illustrated by the rapid decrease in oxygen pressure (Figure 12c), rapid increase in the sample temperature (Figure 12d), rapid increase in radiant heat output (Figure 12e), and rapid increase in sample wear or consumption (Figure 12f). All of these events occur at about 45 seconds. If only the increase in sample temperature was used, a false conclusion may have been drawn that ignition occurred at either 13 or 33 seconds. In reality, these large temperature excursions represent a different phenomenon.



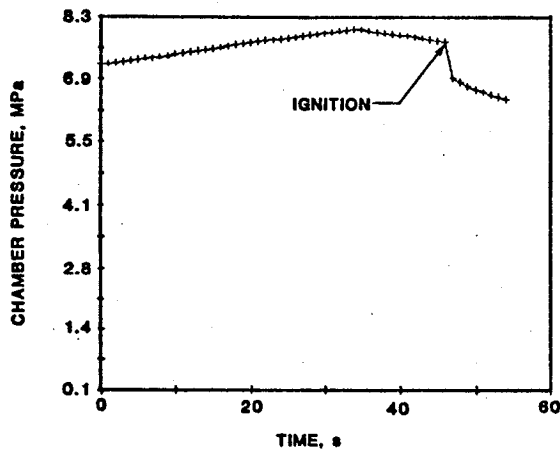
Contact Pressure Calculated from Normal Force

(a)



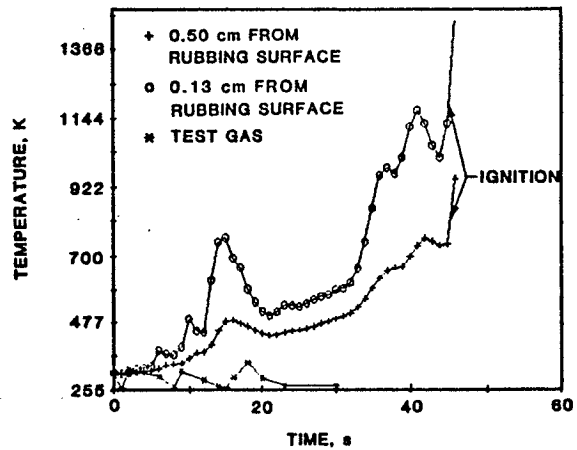
Surface Speed Calculated from Rotational Speed

(b)



Chamber Pressure

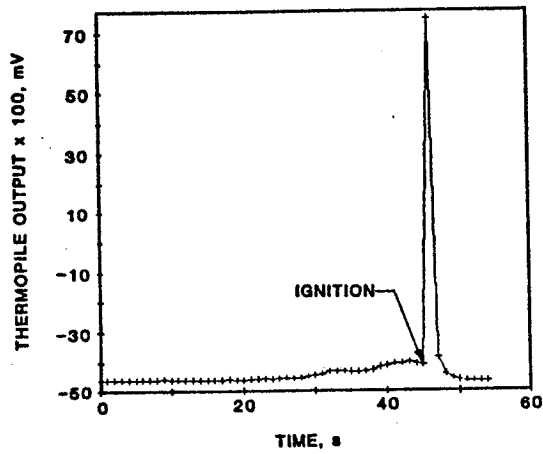
(c)



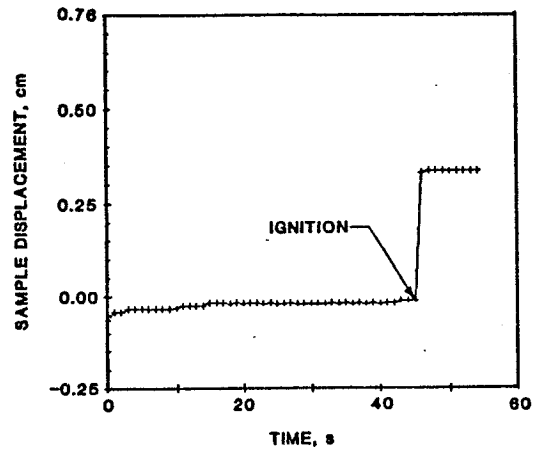
Temperature of Test Sample and Test Gas

(d)

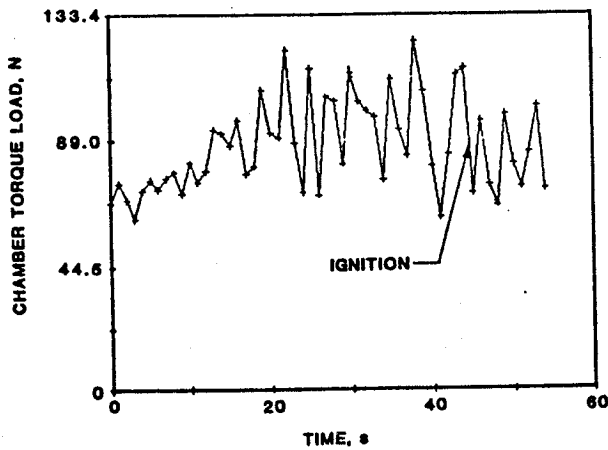
Figure 12: Representative Data From Frictional Heating Test 179  
Conducted on Samples of Monel K-500 at 17,000 rpm and 6.9 MPa



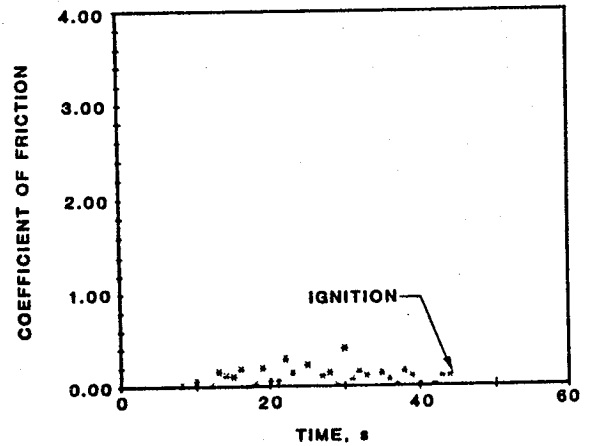
Radiant Energy Output  
(e)



Test Sample Displacement  
(f)



Chamber Torque Load  
(g)



Coefficient of Friction  
Calculated Using the  
Normal Force and the  
Chamber Torque Load  
(h)

Figure 12: Representative Data From Frictional Heating Test 179  
Conducted on Samples of Monel K-500 at 17,000 rpm and 6.9 MPa



A complete set of these data illustrated in Figure 12 are included for each test run in Appendix D. A summary of the initial oxygen pressure, contact pressure application rate, surface velocity, contact pressure at ignition, time to ignition, and Pv product at ignition is presented in Table 1.

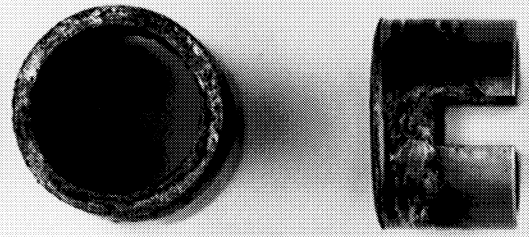
In these frictional heating tests, materials were observed to either ignite or not ignite but fail mechanically (Figure 13). An example of an ignition is represented by type 316 stainless steel in which the posttest view show significant consumption of the samples. Data from the instrumentation showed all characteristics of an ignition that are illustrated in Figure 12. Note that only a portion of the sample was consumed during the burning process which was typical for all material that resulted in ignition. It is believed that the burning process was quenched as oxygen was consumed. Since only a fixed volume of oxygen was available in the chamber, the consumption of oxygen after ignition produced a rapid decrease in the oxygen pressure which served to quench the burning event; see (Figure 12c).

An example of a non-ignition (Figure 13) is represented by zirconium copper (Zi-Cu). The posttest view shows large mechanically deformation of the samples and the data from the instrumentation did not show all the characteristics for an ignition. The only major change in the data was a rapid increase in sample displacement as the samples failed mechanically.

#### 4.4.1.2 Relative Resistance of the Test Materials to Ignition

The ranking criteria used for comparing the relative ignition resistance was the product of the contact pressure (P) and the surface velocity (v) at the point of ignition. Table 2 illustrates the ranking of these materials based on the average Pv products obtained from the three test runs conducted on each material (Table 1). An increase in the average Pv product values indicates a increase in the resistance of materials to ignition by friction heating. Of the materials tested Nickel 200, Inconel 600 and Zi-Cu were the most resistant to ignition. Even though

STATIONARY  
ROTARY  
STAINLESS STEEL 316  
-BURNED-  
AFTER TEST



STATIONARY  
ROTARY  
STAINLESS STEEL 316  
BEFORE TEST

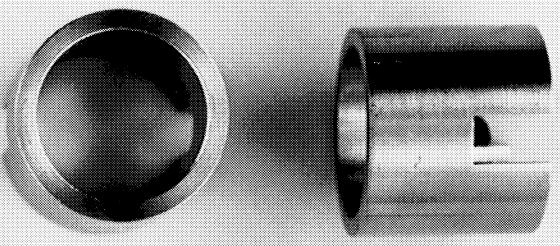


Figure 13: Examples of Results  
of Frictional Heating  
Tests

STATIONARY  
ROTARY  
ZIRCONIUM COPPER  
-FAILED MECHANICALLY-

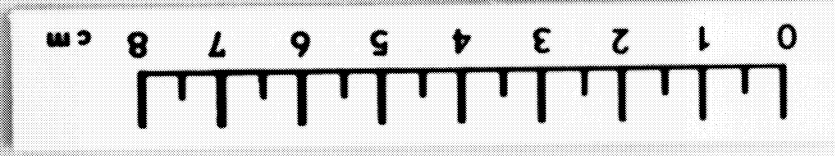
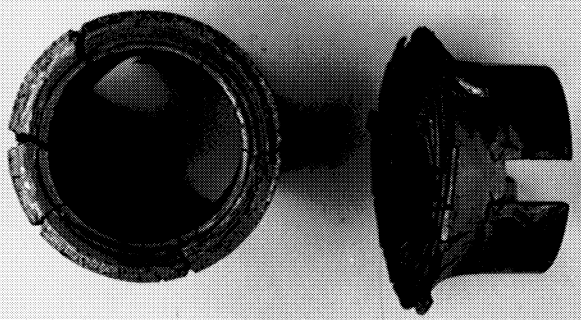


TABLE 1: Summary of Pertinent Test Data for Pairs of Like Materials

Test No.	Initial Oxygen Pressure (MPa)	Contact Pressure Application Rate (N/m <sup>2</sup> /s) x10 <sup>-5</sup>	Surface Velocity at Ignition (m/s)	Contact Pressure at Ignition (N/m <sup>2</sup> ) x10 <sup>-5</sup>	Time to Ignition (s)	Pv Product kW/m <sup>2</sup> x10 <sup>-5</sup>
<u>316 Stainless Steel</u>						
140	7.50	1.10	20.65	26.49	24	0.54
141	7.35	1.24	20.61	35.19	28	0.72
143	7.55	1.17	20.59	30.29	25	0.62
<u>Nickel 200</u>						
142	7.42	1.38	20.47	111.90	80	2.28
144	7.59	1.24	20.28	148.12	120	2.99
161	7.36	1.45	20.25	167.65 <sup>a</sup>	-	3.38
<u>Zirconium Copper (Zi-Cu )</u>						
146	7.56	1.24	20.36	83.48 <sup>b</sup>	-	-
147	7.60	1.24	20.36	107.35 <sup>b</sup>	-	-
148	7.41	0.97	20.36	157.85 <sup>b</sup>	-	-
<u>Invar 36</u>						
149	7.57	1.66	20.34	40.08	24	0.81
150	7.47	1.17	20.34	29.60	25	0.60
154	7.38	1.66	20.34	46.22	27	0.94

TABLE 1: Summary of Pertinent Test Data for Pairs of Like Materials (Continued)

Test No.	Initial Oxygen Pressure (MPa)	Contact Pressure Application Rate (N/m <sup>2</sup> /s) x10 <sup>-5</sup>	Surface Velocity at Ignition (M/s)	Contact Pressure at Ignition (N/m <sup>2</sup> ) x10 <sup>-5</sup>	Time to Ignition (s)	Pv Product kW/m <sup>2</sup> x10 <sup>-5</sup>
<u>Hastelloy x</u>						
151	7.52	1.45	20.34	45.95	32	0.93
152	6.92	1.59	20.34	47.95	29	0.97
153	7.22	1.24	20.31	52.16	41	1.26
<u>Monel 400</u>						
162	7.42	1.59	20.28	70.43	45	1.42
163	7.40	1.52	20.28	71.54	46	1.44
164	7.34	1.59	20.22	76.79	47	1.55
<u>Silicon Carbide</u>						
177	7.83	1.93	20.16	10.2 <sup>b</sup>	-	-
178	7.27	1.52	10.68	24.35 <sup>b</sup>	-	-
<u>Monel K-500</u>						
179	2.25	1.79	20.47	80.24	45	1.63
180	6.97	1.79	20.37	68.30	41	1.39
181	7.24	1.73	20.44	67.71	45	1.63
<u>Inconel 600</u>						
194	7.41	1.38	20.52	134.05	96	2.73
195	7.42	1.52	20.53	97.35	64	1.99
196	7.32	1.52	20.53	141.91	93	2.89

a: No ignition, samples failed mechanically at given contact pressure.

b: No ignition, samples shattered at given contact pressure.

Table 2: Average Heat Rate Per Unit Area (Pv Product) Required for Ignition by Frictional Heating of Pairs of Like Materials

Material	Heat Rate Per Unit Area (Pv Product)	
	$\frac{\text{kW}}{\text{m}^2} \times 10^{-5}$	Standard Deviation
Nickel 200	2.88	0.56
Inconel 600	2.54	0.48
Zirconium Copper (Zi-Cu)*	2.36	0.77
Monel 400	1.47	0.07
Monel K-500	1.46	0.14
Hastelloy X	1.05	0.18
Invar 36	0.78	0.17
Stainless steel 316	0.63	0.09
Silicon carbide (SiC)	**	-

\* Did not ignite, failed mechanically

\*\* Did not ignite, shattered at relatively small contact pressures

Zi-Cu failed mechanically and did not ignite in these tests, the Pv products before the samples failed were large enough to indicate that this material is just as resistant or possibly more resistant to ignition than nickel 200 or Inconel 600. Of the materials tested, Invar 36 and type 316 stainless steel were the least resistant materials to ignition. As a comparison, the Pv products reported by Benz and Stoltzfus (1985) for aluminum 6061-T6 and Ti-6Al-4V at similar conditions were one and two orders of magnitude less, respectively, than the Pv products observed in these tests for the Invar 36 and type 316 stainless steel.

#### 4.4.1.3 Discussion of Test Results

As pointed out earlier, the Pv product measured at the point of ignition represents the heat rate per unit area required from the frictional heating process to ignite the materials. The total energy input is obtained by integrating the Pv product over the time period of the test. However, the contact pressure or the resulting Pv product was steadily increased during the test run until ignition of the material was observed. This change in the Pv product as a function of time can be expressed as shown in Equation 3, and the total frictional energy required for ignition can then be determined by using Equation 4.

$$\frac{d(Pv)}{dt} = (Pv) t^n \quad (3)$$

and

$$Q_f = A \int_{t_0}^{t_i} (Pv) t^n dt \quad (4)$$

where

- A: cross-sectional area at rubbing surface
- Q<sub>f</sub>: frictional energy
- n: time dependent exponent
- t: time
- t<sub>i</sub>: time to ignition
- t<sub>0</sub>: time equal to zero

However, Equation 4 does not represent the fundamental ignition energy for a particular material. Equation 4 does not account for energy that is lost from the samples due to heat transfer and mechanical work and added to the samples due to preignition oxidation. The fundamental ignition energy ( $Q_i$ ) is that energy required to heat the material to a critical temperature ( $T_c$ ), at which point, the rate of oxidation is sufficient to induce ignition of the material; Equation 5.

$$Q_i = m \int_{T_o}^{T_c} C(T) dT \quad (5)$$

where  $C(T)$ : heat capacity as a function of temperature  
 $m$ : mass of the material  
 $T_c$ : critical temperature  
 $T_o$ : initial temperature

The rate of frictional energy ( $dQ_f/dt$ ) required to heat the material to its critical temperature is dependent on the rate of oxidation of the material ( $dQ_{rx}/dt$ ), rate of loss from the material ( $dQ_l/dt$ ), and the rate of any other energy losses to the system ( $dE_m/dt$ ), Equation 6.

$$\frac{dQ_f}{dt} = \frac{dQ_l}{dt} + \frac{dE_m}{dt} - \frac{dQ_{rx}}{dt} \quad (6)$$

The critical temperature is defined in Equation 6 as the temperature that causes  $dQ_f/dt$  to equal zero or  $dQ_l/dt + dE_m/dt = dQ_{rx}/dt$ .

An effort at WSTF has been initiated to develop the necessary models to solve Equation 6.

Based on this previous discussion, the  $P_v$  products given in Table 1 and 2 represent the frictional energy rate per unit area required for ignition of the materials in the WSTF frictional heating apparatus. Different systems or conditions will have different  $P_v$  products required for ignition of these same materials. However, as a relative comparison, the  $P_v$  products listed in Tables 1 and 2 are applicable since the materials were the only major parameter that was changed.

Much can be learned about the ignition process by reviewing the typical data shown in Figure 12. For example, the temperature profile of Monel K-500 during the test run (Figure 12d) indicates the occurrence of large temperature fluctuations prior to ignition. The other data such as contact pressure and surface velocity cannot account for these temperature excursions. The heat source other than frictional heating that could have produced such large temperature excursions was preignition oxidation. Since these temperature increases eventually decay, a mechanism that inhibits oxidation of the material must have also been occurring.

It is well known that metals form protective oxide coatings on their surfaces that can inhibit oxidation (Glassman et al. 1970). If the oxide coating fails, a fresh unoxidized metal surface is exposed and rapid oxidation will occur. The temperature of the material will then increase if the rate of heat generated from the oxidation process exceeds the rate of heat loss from the material. As oxidation of the fresh metal surface occurs, a protective oxide coating will again form and inhibit the oxidation process. The temperature of the material will decrease when the rate of heat loss from the material again exceeds the rate of heat generated by the oxidation process. Since the friction test can apply large stresses to the metal surfaces, the oxide coatings can randomly break throughout a test run and produce multiple temperature excursions prior to ignition. Such multiple temperature excursions are indicated in Figure 12d. The frequency of forming and breaking the oxide coating will increase as temperature increases since the strength of the oxide coating will be reduced at the higher temperatures.

The random breaking of the oxide coatings and its effects on the sample temperatures may account for some of the variations in the Pv products observed in Table 1. In these tests, the contact pressure was continually increased to find the contact pressures required to ignite the sample materials. These unique contact pressures can vary for the same material depending on the state of the oxide coating. For example,



as the contact pressure approaches the value required for ignition of a particular material and if at the same time, the oxide coating breaks, the combination of rapid oxidation and frictional heating can promote ignition of the material. However, if at this same contact pressure, the oxide coating retains its integrity, a greater contact pressure will be required to compensate for the slower inhibited oxidation process.

These results indicate that the ignition characteristics of materials could be improved by selectively altering the properties of the material surfaces to enhance the inhibiting effects on the oxidation process. In addition, these same surface treatments could be used to minimize the frictional heating characteristics of materials by selecting surface treatments that would reduce the coefficient of friction.

#### 4.4.2 Ignition Resistance of Pairs of Different Materials

##### 4.4.2.1 General Comments Concerning the Data

Typical data obtained for each test run were similar to the data obtained for the tests with pairs of like materials, see Figure 12. A complete set of these data for each test run are included in Appendix E.

##### 4.4.2.2 Relative Resistance of the Test Materials to Ignition

The Pv product was again used as the ranking criteria for determining the ignition resistance of materials. The Pv products along with other pertinent data obtained for the three test runs performed on each pair are presented in Table 3. The ranking of these material combinations based on the average Pv products obtained from the three test runs conducted on each combination is presented in Table 4. Monel K-500 rubbed against nickel (ED) exhibited the highest resistance to ignition whereas type 316 stainless steel rubbed against zirconium copper or Monel K-500 exhibited the lowest resistance to ignition. In Figure 14, the Pv products required to ignite the pairs of dissimilar materials

Table 3: Summary of Pertinent Data for Pairs of Different Materials

Test No.	Initial Oxygen Pressure (MPa)	Contact Pressure Application Rate (Nm <sup>2</sup> /s) x10 <sup>-5</sup>	Surface Velocity at Ignition (m/s)	Contact Pressure at Ignition (N/m <sup>2</sup> ) x10 <sup>-5</sup>	Time to Ignition (s)	Pv Product kW/m <sup>2</sup> x10 <sup>-5</sup>
<u>Monel K-500/Monel K-500</u>						
252	7.61	1.31	20.07	86.31	66	1.72
255	7.73	1.38	20.10	90.10	71	1.80
256	7.35	1.31	20.07	84.37	64	1.68
<u>316 SS/Zi-Cu</u>						
257	7.24	1.38	20.04	41.95	31	0.83
258	7.31	1.38	20.10	44.98	34	0.90
259	6.89	1.31	20.13	43.53	33	0.87
<u>316 SS/Monel K-500</u>						
260	7.12	1.38	20.07	39.98	28	1.16
261	7.33	1.11	20.10	36.77	33	1.33
262	6.87	1.31	20.10	36.63	27	1.49
<u>SiC / Invar 36</u>						
263	7.12	1.24	20.01	58.30	58	1.16
264	7.33	1.24	20.10	66.44	53	1.33
265	6.94	1.24	19.98	74.99	58	1.49

Table 3: Summary of Pertinent Data for Pairs of Different Materials (Continued)

Test No.	Initial Oxygen Pressure (MPa)	Contact Pressure Application Rate (Nm <sup>2</sup> /s) x10 <sup>-5</sup>	Surface Velocity at Ignition (m/s)	Contact Pressure at Ignition (N/m <sup>2</sup> ) x10 <sup>-5</sup>	Time to Ignition (s)	Pv Product (kW/m <sup>2</sup> ) x10 <sup>-5</sup>
<u>SiC / Monel K-500</u>						
266 <sup>a</sup>	6.96	1.24	-	-	-	-
267	7.30	1.24	19.98	51.74	43	1.03
268 <sup>a</sup>	6.52	1.24	-	-	-	-
<u>Monel K-500 / Nickel (ED)</u>						
272	7.33	1.38	20.07	88.03	65	1.75
273	7.38	1.17	19.92	82.24	69	1.63
274	7.05	1.17	20.01	67.33	58	1.34

a: SiC samples shattered

Table 4: Average Heat Rate Per Unit Area (Pv Product)  
Required for Ignition by Frictional Heating  
of Pairs of Different Materials

Material Pair (Rotating/Stationary)	Heat Rate Per Unit Area (Pv Product)	
	$\text{kW/m}^2 \times 10^{-5}$	Standard Deviation
Monel K-500/Nickel (ED)	1.57	0.21
SiC/Invar 36	1.33	0.17
SiC/Monel K-500	1.03 <sup>a</sup>	-
316 SS/Zi-Cu	0.87	0.04
316 SS/Monel K-500	0.75	0.03

a: Represents only one test; SiC failed mechanically in two out of the three tests performed.

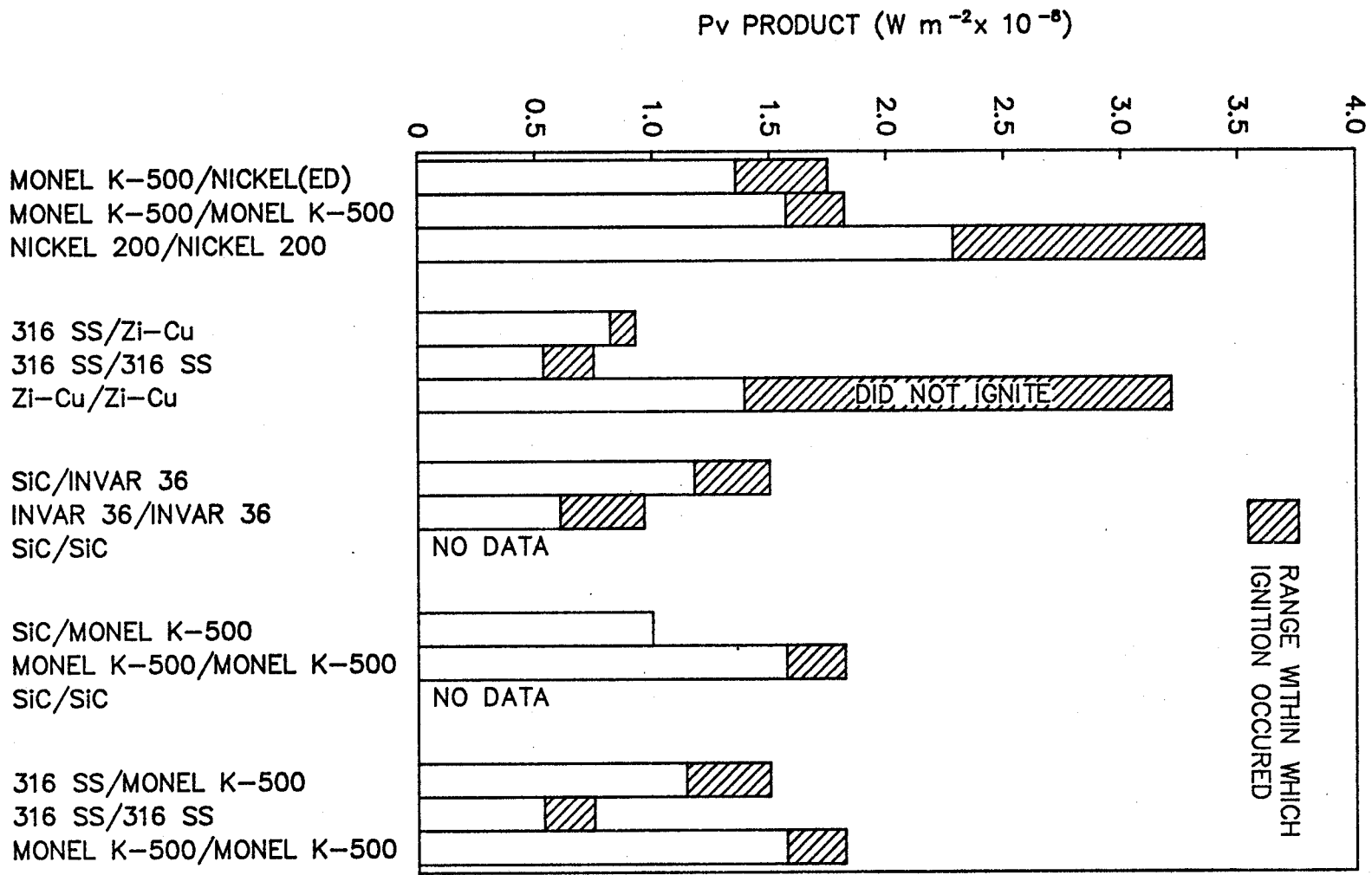
are compared with the Pv products required to ignite the individual materials when rubbed against themselves. In all cases except for silicon carbide (SiC) rubbed against Invar 36, the materials exhibiting the lowest resistance to ignition appeared to dominate the ignition process of the pairs of different materials.

#### 4.4.2.3 Discussion of the Test Results

It was believed at the onset of these tests that the resistance to ignition of the pairs of different materials would reflect the physical and reaction properties of both materials making up the individual pairs. For example, the combination of type 316 stainless steel (low resistance to ignition) and Zi-Cu (high resistance to ignition) represents a case where the differences in the thermal conductivities of the two materials were substantial; the thermal conductivity of Zi-Cu is as much as one order of magnitude greater than the thermal conductivity of type 316 stainless steel. The high thermal conductivity of Zi-Cu should increase the heat loss (conduction) from the rubbing surface of the type 316 stainless steel and should cause an increase in the Pv product required to ignite type 316 stainless steel. The results (Figure 14) indicate that there was approximately a 38 percent increase in the Pv product required to ignite type 316 stainless steel when rubbed against Zi-Cu. The other pairs of different materials consisted of combinations in which the differences in the thermal conductivity were small. The scatter in the data made it impossible to determine what effects smaller differences in thermal conductivity would have on the ignition process. The effects of other physical properties, such as heat capacity, coefficient of friction were not evident in these tests. These tests indicated that the reaction properties of the material least resistant to ignition appeared to dominate the ignition properties of the pairs.

The results for the combination of SiC and Invar 36 (Figure 14) did not follow the general trend as observed for the other combinations of pairs of different materials. When SiC was rubbed against Invar 36, a larger resistance to ignition resulted than when Invar 36 was rubbed against

Figure 14: Pv Products Required to Ignite Pairs of Different Materials



itself. No data were obtained for SiC rubbed against itself, but the results for the combination of SiC and Monel K-500 indicate that the resistance to ignition of SiC is probably similar to that of Invar 36.

#### 4.4.3 Effect of Oxygen Pressure on the Ignition of Materials

In these tests, the effect of oxygen pressure on the sample temperature and coefficient of friction was evaluated using Monel K-500. Two tests with new samples were conducted in which the contact pressure and surface velocities were maintained constant while the oxygen pressure was increased from 0.69 MPa (100 psia) to 6.89 MPa (1000 psia) and then to 20.7 MPa (3000 psia).

The results from several tests are also included in which carbon steel 1015 samples were tested in oxygen and nitrogen atmospheres at 0.69 MPa (100 psia), 6.89 MPa (1000 psia), and 20.7 MPa (3000 psia). In these tests, the normal force applied to the samples was increased at a rate of 31 N/s (7.0 lb<sub>f</sub>/s). The purpose of these tests was to determine the effects of pressure on frictional heating and ignition of materials.

##### 4.4.3.1. General Comments Concerning the Data

Typical data obtained for these tests were similar to the data illustrated in Figure 12. A complete set of these data for each test run is given in Appendix F. Pertinent data are summarized in Table 5 for each of the test runs with Monel K-500 samples and the change in equilibrium sample temperature and coefficient of friction are illustrated in Figures 15 and 16. Sample temperature increase as a function of pressure for the carbon steel 1015 samples as illustrated in Figure 17 for oxygen and nitrogen atmospheres.

##### 4.4.3.2 Description of the Test Results

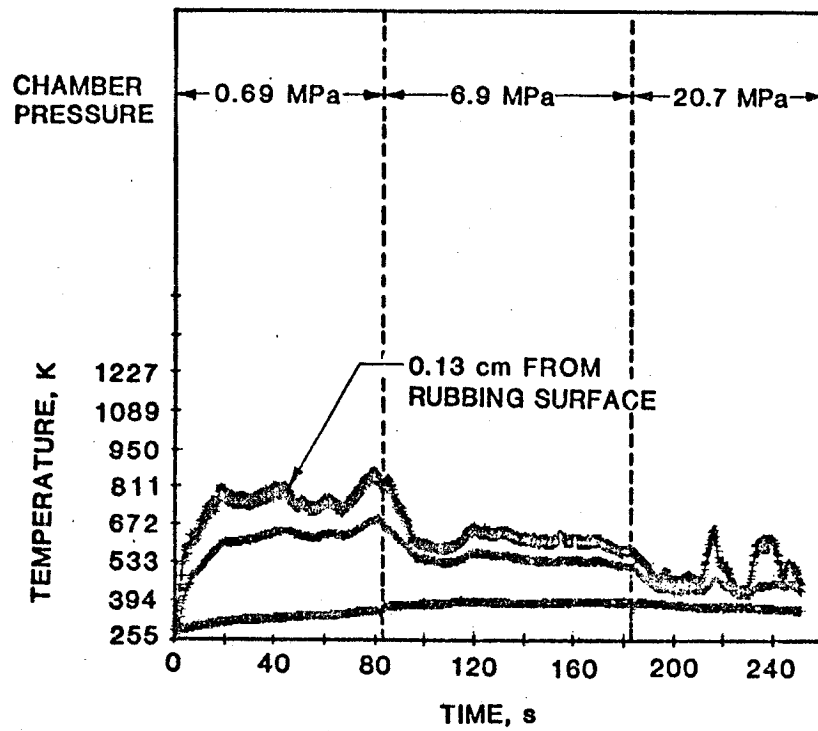
The results from both test runs with Monel K-500 samples indicated that as oxygen pressure was increased, the sample temperatures decreased, and

Table 5: Summary of Pertinent Data for the Effects of Oxygen Pressure on Frictional Ignition of Materials

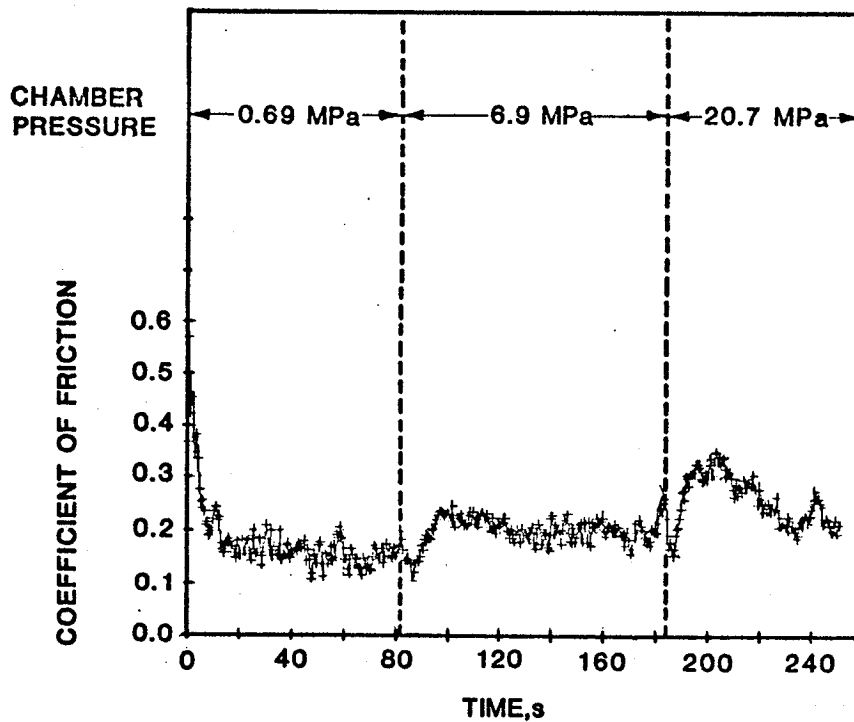
Average Surface Speed (m/s)	Average Contact Pressure (N/m <sup>2</sup> )	Initial Oxygen Pressure (kPa)	Average * Equilibrium Temperature (k)	Average Coefficient of Friction
Test # 236: Monel K-500				
5.98;SD:0.01	2.03;SD:0.13	0.69	754;SD:29	0.16;SD:0.07
5.98;SD:0.01	1.99;SD:0.11	6.89	607;SD:20	0.21;SD:0.05
5.98;SD:0.01	1.97;SD:0.04	20.7	511;SD:55	0.27;SD:0.09
Test # 237: Monel K-500				
5.98;SD:0.01	2.22;SD:0.07	0.69	811;SD:16	0.11;SD:0.12
5.98;SD:0.01	2.18;SD:0.06	6.89	613;SD:40	0.14;SD:0.05
5.98;SD:0.01	2.14;SD:0.05	20.7	488;SD:25	0.17;SD:0.08

\*: Temperature measured at 0.13 cm from rubbing surface  
SD: Standard Deviation



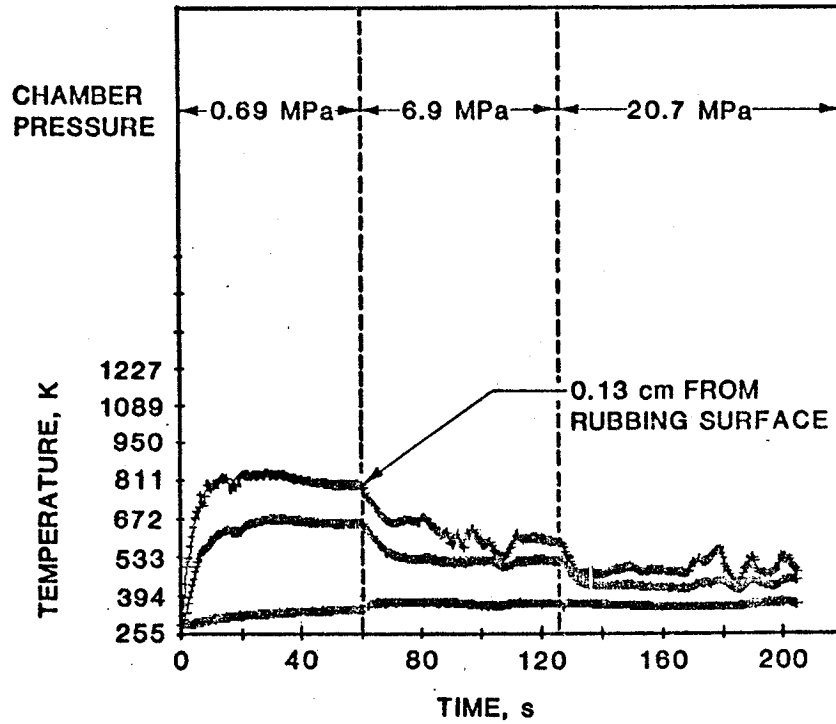


(a) Sample Temperature as a Function of Time and Oxygen Pressure

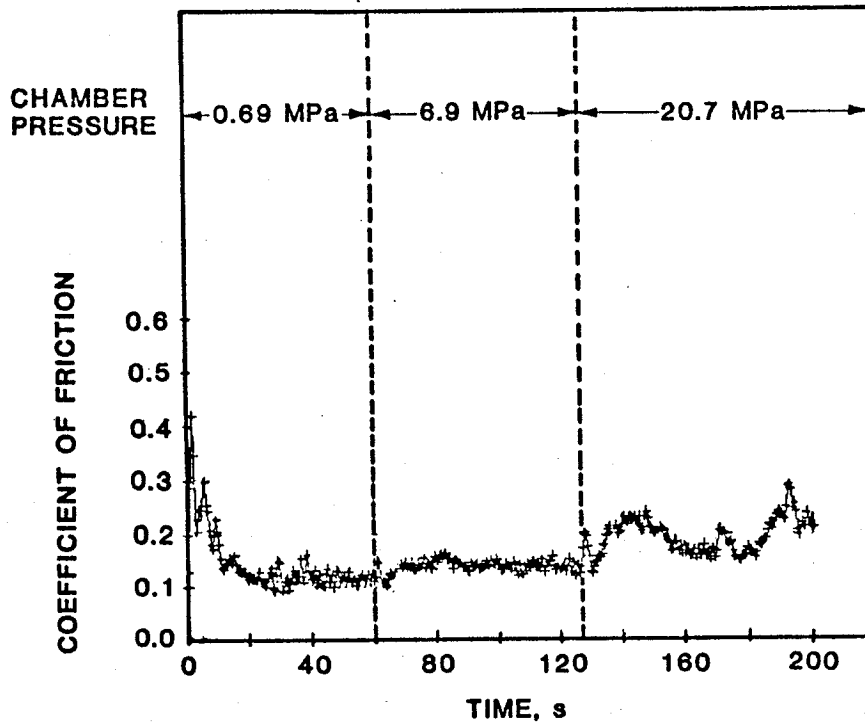


(b) Coefficient of Friction as a Function of Time and Oxygen Pressure

Figure 15: Effects of Oxygen Pressure on the Sample Temperature and Coefficient of Friction for Monel K-500 (Test #236)



(a) Sample Temperature as a Function of Time and Oxygen Pressure



(b) Coefficient of Friction as a Function of Time and Oxygen Pressure

Figure 16: Effects of Oxygen Pressure on the Sample Temperature and Coefficient of Friction for Monel K-500 (Test #237)

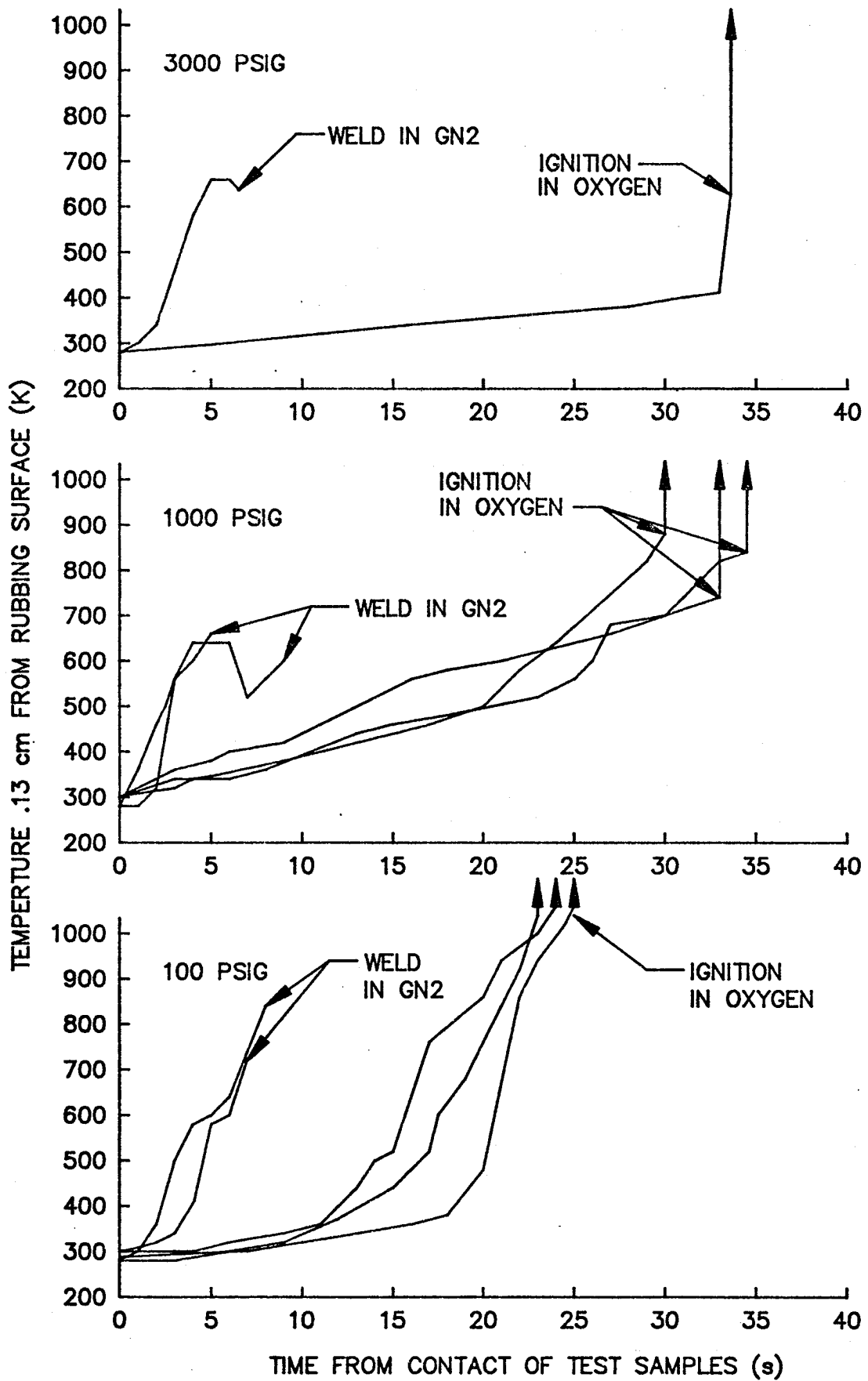


Figure 17: Temperature of 1015 Carbon Steel When Frictionally Heated in GN<sub>2</sub> and Oxygen at 100, 1000, and 3000 psig

the coefficients of friction increased (Figures 15 and 16). The magnitudes of these changes are summarized in Table 5. In test number 236, the average sample temperature decreased approximately 32 percent and the average coefficient of friction increased approximately 69 percent as oxygen pressure was increased from 0.69 to 20.7 MPa. In test number 237 for the same increase in oxygen pressure, the average sample temperature decreased approximately 40 percent and the average coefficients of friction increased approximately 55 percent.

The results for the carbon steel 1015 tests indicated that the sample temperature increased at much faster rates when samples were rubbed in a nitrogen atmosphere as opposed to in an oxygen atmosphere. An increase in oxygen pressure produced significant decreases in the rates at which the sample temperature increased. The effects of increasing nitrogen pressure on the increase in sample temperatures were inconclusive from these tests. This is probably due to the large tendency for the samples to weld. These results also indicated that the temperature where rapid oxidation and subsequent ignition of the samples decreased as oxygen pressure was increased.

#### 4.4.3.3 Discussion of the Test Results

These tests were designed to identify the causes for the increase in the Pv products required for ignition as oxygen pressure was increased, as discussed in Section 4.1. An increase in convective heat loss from the samples and a decrease in the coefficient of friction were believed to be the major influencing factors. In the case of the coefficient of friction, it was postulated that at higher oxygen pressures the formation of oxide layers between the rubbing sample surfaces would be enhanced thereby causing the coefficient of friction to decrease. The rate of frictional heating would decrease, and a greater Pv product would be required for ignition. In the case of an increase in convective heat transfer from the sample, a greater input of frictional energy (increase in the Pv product) would be required for ignition to compensate for the increased rate of heat loss.

The results for Monel K-500 samples indicated that the equilibrium sample temperature decreased and the coefficient of friction increased as oxygen pressure was increased. These results imply that the decrease in the sample temperature was caused by an increase in convective heat loss since the coefficient of friction was observed to increase in these tests. The results from the carbon steel 1015 tests also support this same general conclusion. Thus, as oxygen pressure is increased, greater frictional energies (larger  $Pv$  products) are required to raise the temperature of the sample materials to their ignition temperatures.

In theory, an increased oxygen pressure, besides increasing the heat loss from sample materials, can increase the rate of oxidation. The effects of oxygen pressure on the oxidation rate of metallic materials are dependent upon the type of oxide coatings that form; absorption controlled,  $(P_{Ox})^{1/2}$ , and diffusion controlled,  $(P_{Ox})^{1/n}$ , where  $n$  can vary between 5 and 8 (Kofstad 1966). The effects of oxygen pressure on laminar free convection and turbulent free convection are approximately  $(P_{Ox})^{1/2}$  and  $(P_{Ox})^{2/3}$  respectively (Rohsenow and Hartnett 1973).

Schmidt and Forney (1975) reviewed the ignition temperatures of metals and alloys as a function pressure obtained in heated bombs. The ignition temperatures are observed to increase, decrease, or remained the same as oxygen pressure is increased for different metals and alloys. Laurendeau (1969) provided evidence that ignition temperatures of metals and alloys are dependent on the characteristics of the oxide coatings (protective or non-protective) that form during the pre-ignition oxidation process. Protective oxide coatings induce metals and alloys to undergo diffusion controlled oxidation whereas non-protective oxide coatings allow metals and alloys to undergo absorption controlled oxidation. As shown previously, diffusion controlled oxidation is less dependent on oxygen pressure than absorption controlled oxidation. This implies that metals and alloys following absorption controlled oxidation should exhibit ignition temperatures that are more dependent on pressure than metals and alloys following diffusion controlled oxidation.

Comparing the effects of pressure on the ignition temperatures of the carbon steels and the Monels can provide insight into the type of controlling oxidation processes and the properties of the oxide coatings of these alloys. The ignition temperatures as a function of oxygen pressure for these alloys are given in Table 6 (Schmidt and Forney 1975). The carbon steels exhibit a decrease in their ignition temperatures as pressure is increased whereas the ignition temperatures of the Monels appear to be independent of pressure. The pressure effects on the ignition temperatures of the carbon steels imply that these alloys may not form totally protective oxide coatings and indicates that absorption controlled oxidation may play a role in the oxidation process. On the other hand, the pressure effects on the ignition temperatures of the Monels imply that these alloys form protective oxide coatings and indicates that diffusion controlled oxidation plays a major role in the oxidation process.

The use of these alloys in oxygen system normally involve dynamic conditions and the stresses placed on the oxide coatings such as those experienced in a rubbing process are a major concern. The bulk ignition temperatures as a function of oxygen pressure for carbon steel 1015 and Monel 400 when exposed to friction heating tested are given in Table 7. The temperature in these tests were measured at 0.13 cm from the rubbing surfaces. The bulk ignition temperature of carbon steel 1015 appears to decrease significantly as pressure is increased whereas the bulk ignition temperature of Monel 400 is observed to remain essentially constant as pressure is increased. Because the temperature of the rubbing surfaces was not measured in these tests, the absolute values for these ignition temperatures will be lower than the ignition temperatures reported by Schmidt and Forney (1975). However, the same general conclusions can be made about the relative changes that are observed in these ignition temperatures. Monel 400 when exposed to a rubbing process appeared to retain its protective oxide coating since increasing oxygen pressure had little effect on the ignition temperature. The oxide coating that formed on carbon steel 1015 appeared to loose some of its protective characteristics when exposed to a rubbing process since the ignition

Table 6: Ignition Temperatures of Carbon Steels and Monel Alloys Determined in Heated Bomb Tests (Schmidt and Forney 1975)

Pressure (MPa)	Ignition Temperature (K)
<u>Carbon Steels</u>	
0.69	1370 - 1460
6.9	1290 - 1340
10.1	1270 - 1320
<u>Monels</u>	
0.69	Approximately 1470
6.9	Approximately 1470
10.1	Approximately 1470

Table 7: Sample Temperature and Pv Product Required for Ignition as a Function of Pressure

Pressure (MPa)	Average Ignition Temperature (K)	Pv Product (kW/M <sup>2</sup> )
<u>Carbon Steel 1015</u>		
0.69	1100	$0.21 \times 10^5$
6.9	750 - 870	$0.26 \times 10^5$
20.7	480	$0.31 \times 10^5$
<u>Monel 400</u>		
6.9	1150	$1.17 \times 10^5$
13.8	1115	$1.45 \times 10^5$
20.7	1125	$2.21 \times 10^5$

temperature decreased more dramatically as compared with the heated bomb tests. This would imply the oxidation process of carbon steel is becoming more dependent on absorption controlled oxidation.

The Pv products required for ignition of carbon steel 1015 and Monel 400 in the frictional heating tests are also included in Table 6. Monel 400 required a 90 percent increase in the Pv product for ignition when oxygen pressure was increased from 6.9 MPa (1000 psia) to 20.7 MPa (3000 psia). Carbon steel 1015 required only a 19 percent increase in its Pv product required for ignition for the same increase in oxygen pressure. Since the oxidation process for Monel 400 appeared to be diffusion controlled, increasing oxygen pressure caused a smaller increase in the oxidation rate (less heat generation) when compared to carbon steel 1015 which appeared to be approaching absorption controlled oxidation. Therefore, when oxygen pressure was increased, in the case of Monel 400, convective heat transfer may have had a major role in the ignition process since a large portion of the oxygen was not involved in producing heat via oxidation. Larger frictional energies were then required for ignition of Monel 400 to compensate for the increase in convective heat loss and the small increase in the oxidation rate as oxygen pressure was increased. In the case of carbon steel 1015, a similar increase in oxygen pressure would have the same effect on increasing convective heat transfer as with Monel 400. But the larger increase in the oxidation rate experienced by carbon steel 1015, as it approaches absorption controlled oxidation, implies that less frictional energy was required to reach its ignition temperature.

The importance of these observations, if they hold true for the general case, is that the resistance to ignition of metals and alloys such as the carbon steels can be increased if techniques can be developed to duplicate the characteristics of the protective oxide coatings afforded by the Monels. Ion implantation, dopants, and inert coatings are possible techniques that may result in the generation of surfaces that are superior to the original surfaces of metals and alloys in inhibiting oxidation.



## 5.0 CONCLUSIONS

Several materials were subjected to particle impact and to frictional heating tests in high pressure oxygen. Their relative resistances to ignition were determined.

In the particle impact test, nickel 200, Monel 400, and silicon carbide did not show any evidence of any type of burning and thus were rated as materials with the highest resistances to ignition. Monel 400 and zirconium copper showed only slight surface burning and were rated slightly less resistant to ignition than the above-mentioned materials. Hastelloy X exhibited partial burning and quenched before the entire sample was consumed, whereas Invar 36 and type 316 stainless steel exhibited burning in which the entire sample was consumed. Hastelloy X, Invar 36, and type 316 stainless steel were rated as materials least resistant to ignition. Tests conducted to determine if rupturing of a target material by impacting particles would enhance ignition were inconclusive.

In the frictional heating tests, the relative resistances to ignition were based on the product of the contact pressure (P) and surface velocity (v) required for ignition of the materials. When pairs of the same materials were rubbed, nickel 200, Inconel 600, and zirconium copper exhibited the highest resistances to ignition with average Pv products in excess of  $2 \times 10^5$  kW/m<sup>2</sup>. Monel 400 and Monel K-500 exhibited the next highest resistances to ignition with average Pv products of  $1.47 \times 10^5$  kW/m<sup>2</sup> and  $1.46 \times 10^5$  kW/m<sup>2</sup>, respectively. Hastelloy X, Invar 36, and type 316 stainless steel exhibited the lowest resistances to ignition with Pv products of  $1.05 \times 10^5$  kW/m<sup>2</sup>,  $0.78 \times 10^5$  kW/m<sup>2</sup>, and  $0.63 \times 10^5$  kW/m<sup>2</sup>, respectively.

When pairs of different materials were exposed to frictional heating, Monel K-500 rubbed against nickel (electra-deposited) exhibited the highest resistance to ignition with an average Pv product of  $1.57 \times 10^5$  kW/m<sup>2</sup>. The combinations of silicon carbide rubbed against Invar 36 and

Monel K-500 exhibited the next highest resistances to ignitions with average Pv products of  $1.33 \times 10^5$  and  $1.03 \times 10^5$  kW/m<sup>2</sup>, respectively. Material combinations exhibiting the lowest resistances to ignition were type 316 stainless steel rubbed against zirconium copper with an average Pv product of  $0.87 \times 10^5$  kW/m<sup>2</sup> and type 316 stainless steel rubbed against Monel K-500 with an average Pv product of  $0.75 \times 10^5$  kW/m<sup>2</sup>.

Tests were conducted to determine the effects of increased oxygen pressure on the frictional heating properties of materials. In these tests, pairs of Monel K-500 samples were rubbed at a constant Pv product and only oxygen pressure was varied. The equilibrium sample temperature decreased and the coefficient of friction increased as oxygen pressure was increased from 0.69 to 20.7 MPa. An increase in the convective heat transfer from the sample was concluded as being responsible for the decrease in the equilibrium sample temperature as oxygen pressure was increased.

Frictional heating tests were also performed on carbon steel 1015 samples in oxygen and nitrogen atmospheres at various pressures. Tests conducted in oxygen were taken to ignition. Heating of the samples occurred at a much faster rate in the nitrogen atmosphere than in the oxygen atmosphere. It was concluded that in an oxygen atmosphere the coefficient of friction was reduced due to the formation of oxide layers at the rubbing surfaces. As oxygen pressure was increased, the bulk ignition temperature decreased and the Pv product required for ignition increased.

## References

Benz, F. J., R. Williams, and Armstrong, D., Ignition of Metals and Alloys by High-Velocity Particles. Paper presented at the Symposium on Flammability and Sensitivity of Materials in Oxygen-Enriched Atmospheres, April 1985.

Benz, F. J., and C. V. Bishop. Evaluation of Pressure Effects in the WSTF Friction Rubbing Test System. NASA TP-WSTF-356, January 1984.

Benz, F. J., J. Homa, and R. C. Shaw. Propagation Rates of Various Metals and Alloys in Oxygen. Paper presented at the Symposium on Flammability and Sensitivity of Materials in Oxygen-Enriched Atmospheres, April 1985.

Benz, F. J. and J. Stoltzfus. Ignition of Metals and Alloys in Gaseous Oxygen by Frictional Heating. Paper presented at the Symposium on Flammability and Sensitivity of Materials in Oxygen-Enriched Atmospheres, April 1985.

Clark, A. F. and T. G. Hurst, "A Review of the Compatibility of Structural Materials with Oxygen," AIAA Journal, Vol. 12, No. 4, April 1974, pp. 441-454.

Cooper, L. P., Advanced Propulsion Concepts for Orbital Transfer Vehicles. NASA TM-83-419, June 1983.

Glassman, I., A. M. Mellor, H. F. Sullivan, and N. M. Laurendeau, "A Review of Metal Ignition and Flame Models," Conference Proceedings 52, NASA AGARD Annual Meeting. Neuilly-Sur-Seine, France, Feb. 1970. pp. 19 (1-30).

Jenny, R. and H. R. Wyssmann, "Friction-Induced Ignition in Oxygen," Flammability and Sensitivity of Materials in Oxygen-Enriched Atmospheres. STP 812. American Society for Testing and Materials, Philadelphia, 1983. pp. 150-166.

Kofstad, P., High Temperature Oxidation of Metals, Wiley, New York. 1966.

Lapin, A., "Liquid and Gaseous Oxygen Safety Review," Vol. I-IV. NASA-CR-120922. APCI TM184, NASA Lewis Research Center, Cleveland, OH, June 1972.

Laurendeau, N. M., The Ignition Characteristics of Metals in Oxygen Atmospheres, Tech. Rept. No. 851, Dept. of Aerospace and Mechanical Sciences, Princeton University, NJ, Oct. 1963.

Naegeli, J. P., "What Triggers Oxygen Turbo Compressor Fires," Proceedings. Oxygen Compressors and Pumps Symposium, Compressed Gas Association, Atlanta, GA 1971. pp. 35-38.

Nihart, G. J. and C. P. Smith, "Compatibility of Metals with 7500 psi Oxygen." Report AD 608 260, Union Carbide, Linde Division, Tonawanda, NY. Oct. 1964.

Natrella, M. G., Experimental Statistics. National Bureau of Standard Handbook 91, August 1963.

Rohsenow, W. M. and J. P. Hartnett, Eds., Handbook of Heat Transfer. McGraw-Hill Book Co., New York, 1973.

Schmidt, H. W. and Forney, D. F., ASRDI Oxygen Technology Survey, Volume IX: Oxygen Systems Engineering Review, NASA SP-3090, NASA, Washington, DC, 1975.

Thayer, R. M. "Proposed Program for Combustibility Tests." In study of Handling Standards and Safety Criteria for Liquid and Gaseous Oxygen Systems, Section 3.0. Prepared for NASA Lewis Research Center by Union Carbide Corp., Linde Division, June 1971.

## APPENDIX A

### Determination of the Test Sample Temperature in the Particle Impact Tester

In the particle impact test the temperature of the oxygen at the inlet to the test chamber was measured but the temperature of the test sample was not. In order to determine the temperature of the test sample relative to the temperature of the oxygen, a series of calibration tests were performed. The test chamber was modified as shown in Figure A-1. A test fixture which replaced the test sample was made. A port was placed in the test fixture in which a thermocouple could be mounted to measure the stagnation temperature of the oxygen at a location coincident until the surfaces of the test sample in the original test chamber.

Flow checks were performed in which heated oxygen was flowed through the test chamber at conditions similar to the testing done in this program and the temperature chamber inlet (A) and at the test sample locations (B) were compared. The results of these tests are shown in Figure A-2. It was found that the temperature as measured at the test sample ranged from 44 to 74 °F greater than those measured at the inlet to the test chamber.

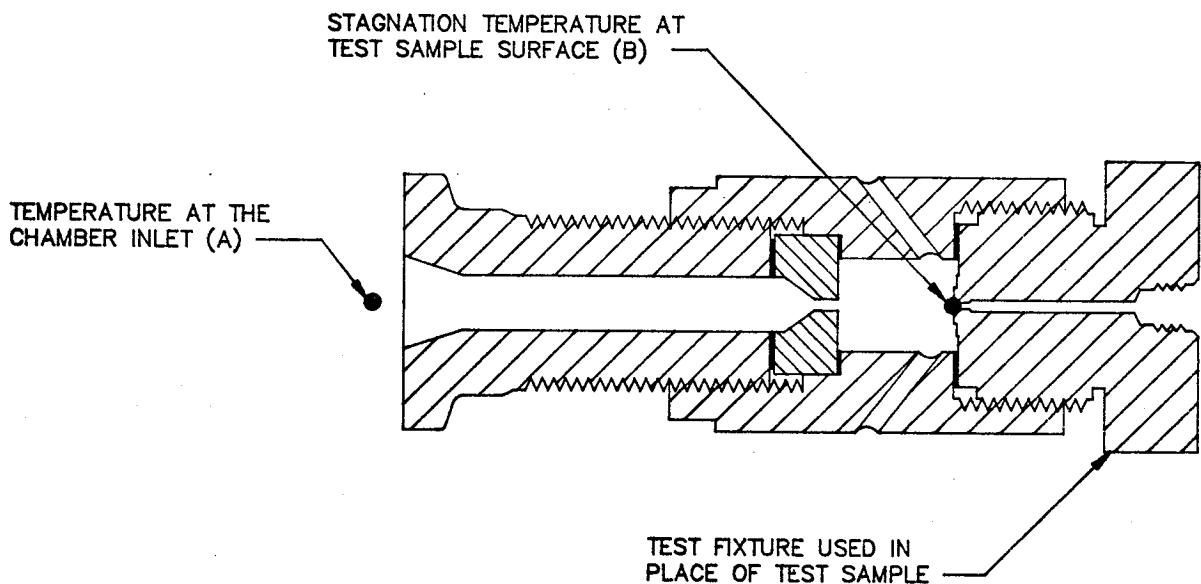


Figure A-1: Modified Particle Impact Chamber Used to Determine Temperature at Surface of Test Sample

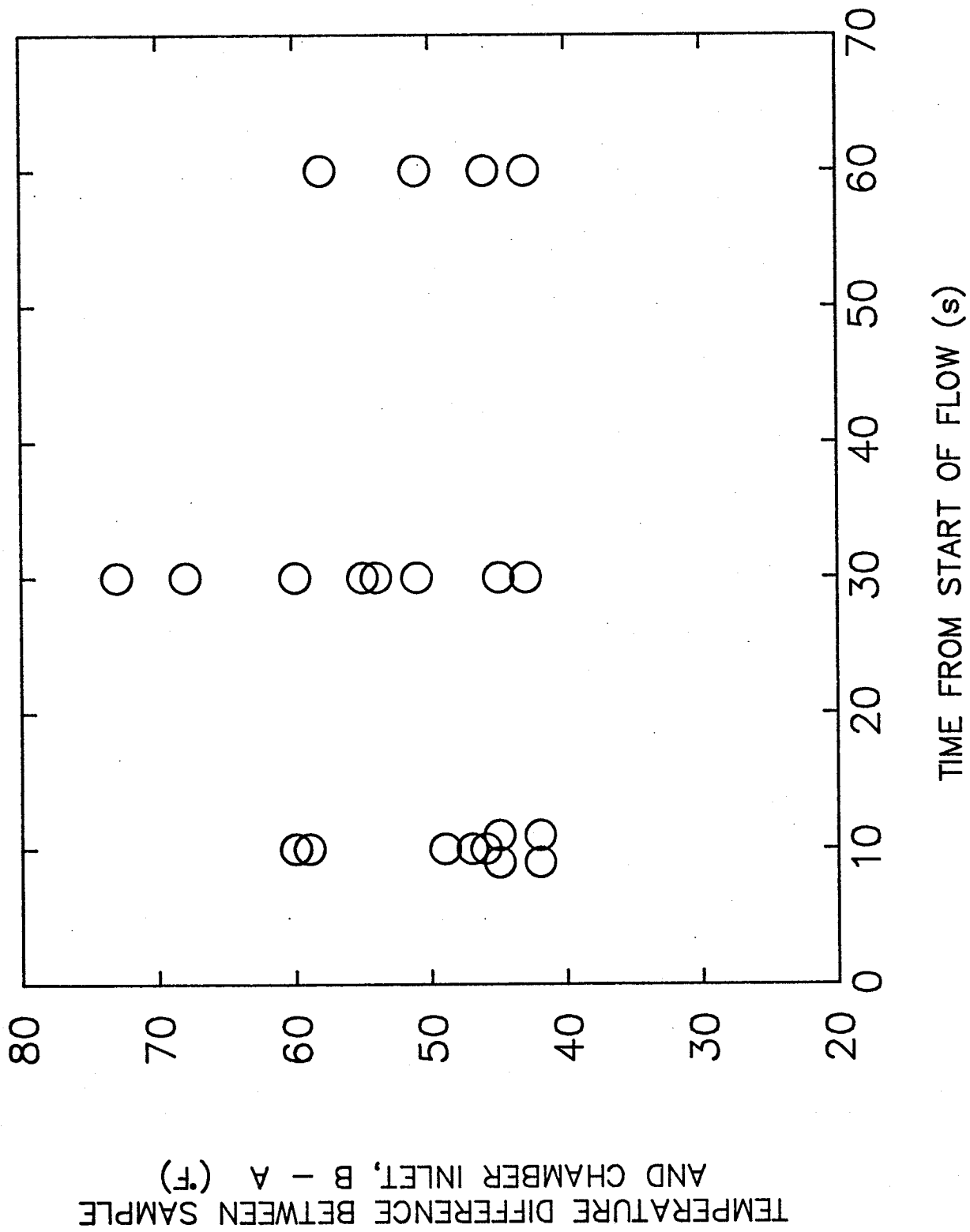


Figure A-2. Results of Test to Determine the Temperature Difference Between the Test Sample Surface and the Test Chamber Inlet

## APPENDIX B

### Estimation of Minimum Particle Velocity by a Dent-Block Comparison Test

In order to make an estimate of the particle velocity in the particle impact test a dent block comparison test was done. Several tests were done in the gaseous oxygen high flow test facility in which a 1600  $\mu\text{m}$  diameter particle was impacted against a copper impact plate at ambient temperature. In each of these tests a dent with a diameter ranging from 1100 to 1200  $\mu\text{m}$  was made in the copper impact plate. Next, several drop tower tests were performed in the laboratory in which a weighted aluminum particle was dropped onto a copper plate from a known height. The aluminum particle was held in a chuck which was commonly used in a hardness tester as shown in Figure B-1. The particle and the impact plate were identical to the ones used in the particle impact test. In the drop tower the dents that were made ranged from 1100 to 1200  $\mu\text{m}$  in diameter.

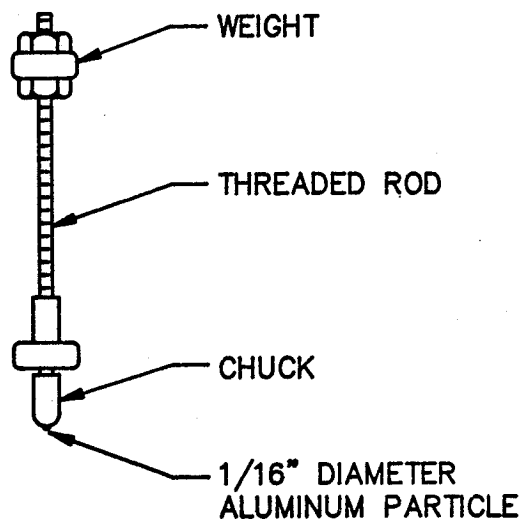


Figure B-1: Plummet Used in Dent Block Comparison Test

Two assumptions were made in order to calculate the particle velocity based on the data obtained from the tests described above. First, the work done making the dent in the particle impact test,

$$E_{PI} = 1/2 m_p g (V_{P2}^2 - V_{PI}^2) \quad (1)$$

was equal to the work done making the dent in the drop tower test,

$$E_{DT} = 1/2 m_w g (V_{W2}^2 - V_{W1}^2) \quad (2)$$

or,

$$E_{PI} = E_{DT} \quad (3)$$

for dents that were the same size. Where,

$E_{PI}$  = Work done making the dent in the particle impact test [=] ft lbf

$m_p$  = Mass of 1600 um diameter aluminum particle [=] slugs

$g$  = 32.174 [=] lbf s<sup>2</sup> lbm<sup>-1</sup> ft<sup>-1</sup>

$V_{P2}$  = Velocity of particle as it rebounds from impact [=] ft s<sup>-1</sup>

$V_{P1}$  = Velocity of particle prior to impact [=] ft s<sup>-1</sup>

$E_{DT}$  = Work done making the dent in the drop tower test [=] ft lbf

$m_w$  = Mass of the weighted particle used in the drop tower test [=] slugs

$V_{W2}$  = Velocity of the weighted particle after impact [=] ft s<sup>-1</sup>

$V_{W1}$  = Velocity of the weighted particle prior to impact [=] ft s<sup>-1</sup>

Since  $W = mg$  we have,

$$E_{PI} = 1/2 W_p (V_{P2}^2 - V_{PI}^2) \quad (4)$$

and,

$$E_{DT} = 1/2 W_w (V_{W2}^2 - V_{W1}^2) \quad (5)$$



where,

$W_p$  = Weight of particle used in particle impact test [=] lbf

$W_w$  = Weight of weighted particle used in drop tower test [=] lbf

The second assumption made was that the coefficient of restitution for the aluminum particle and the copper plate was the same in the particle impact test as it was in the drop tower test. Another way of stating this is that neither the aluminum or the copper materials were strain rate dependent. Since, in the particle impact test, the copper impact plate was stationary, then

$$e_{pI} = \frac{V_{p2}}{V_{pI}} \quad (6)$$

where,

$e_{pI}$  = coefficient of restitution in the particle impact test [=]  
dimensionless

For the drop tower, we know that

$$V_{w1} = (2g_c h_1)^{\frac{1}{2}} \quad (7)$$

and,

$$V_{w2} = (2g_c h_2)^{\frac{1}{2}} \quad (8)$$

where,

$h_1$  = height from which the weighted particle was dropped [=] ft

$h_2$  = height of rebound of the weighted particle [=] ft

$g_c$  = gravitational constant [=] 32.2 ft s<sup>-2</sup>

The coefficient of restitution for the drop tower test was

$$e_{DT} = \frac{V_{w2}}{V_{w1}} \quad (9)$$

Substituting equation 7 and 8 into 9 gives,

$$e_{DT} = \left( \frac{h_2}{h_1} \right)^{\frac{1}{2}} \quad (10)$$

and from assumption two we have,

$$e_{PI} = e_{DT} \quad (11)$$

Therefore,

$$\frac{V_{P2}}{V_{P1}} = \left( \frac{h_2}{h_1} \right)^{\frac{1}{2}} \quad (12)$$

or,

$$V_{P2} = V_{P1} \left( \frac{h_2}{h_1} \right)^{\frac{1}{2}} \quad (13)$$

Now, from equation 3, 4 and 5, we have

$$1/2 W_w (V_{W2}^2 - V_{W1}^2) = 1/2 W_p (V_{P2}^2 - V_{P1}^2) \quad (14)$$

By substituting equation 7, 8 and 13 into equation 14, we obtain

$$\begin{aligned} 1/2 W_w (2g_c h_2 - 2g_c h_1) &= 1/2 W_p (V_{P1}^2 \cdot \frac{h_2}{h_1} - V_{P1}^2) \\ W_w g_c (h_2 - h_1) &= 1/2 W_p V_{P1}^2 \left( \frac{h_2}{h_1} - 1 \right) \\ V_{P1} &= \left( 2g_c \frac{W_w}{W_p} h_1 \frac{h_2 - h_1}{\frac{h_2}{h_1} - 1} \right)^{\frac{1}{2}} \\ V_{P1} &= \left( 2g_c \frac{W_w}{W_p} h_1 \right)^{\frac{1}{2}} \end{aligned} \quad (15)$$

Now for a dent size of 1125  $\mu\text{m}$  it was found that,

$$\begin{aligned}W_w &= 3.33 \times 10^{-2} \text{ lbf} \\W_p &= 1.278 \times 10^{-5} \text{ lbf} \\h_1 &= 4.075 \text{ ft}\end{aligned}$$

Substituting into equation 15, we have

$$\begin{aligned}V_{PI} &= 2 (32.2) \frac{3.83 \times 10^{-2} (4.075)^{\frac{1}{2}}}{1.278 \times 10^{-5}} \\&= 887 \text{ ft s}^{-1}\end{aligned}$$

Several different weights and drop heights were used and it was found the estimated particle velocity ranged from 853 to 887  $\text{ft s}^{-1}$ .